

Multi-messenger constraints on the dark matter interpretation of the Fermi-LAT Galactic center excess

Mattia Di Mauro

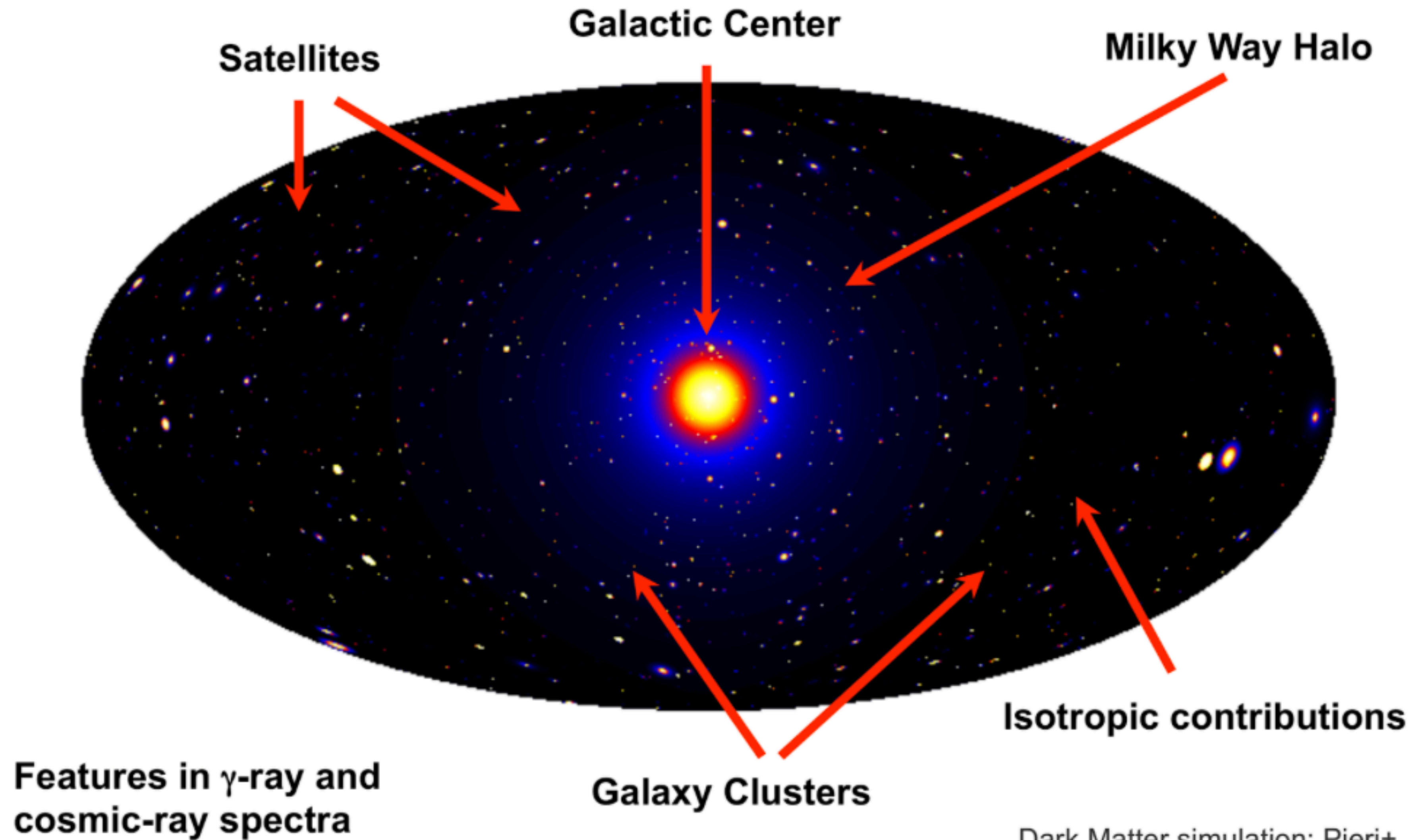


ICHEP, 6-13 July 2022, Bologna

Background image: ESO
Central image: Fermi-LAT

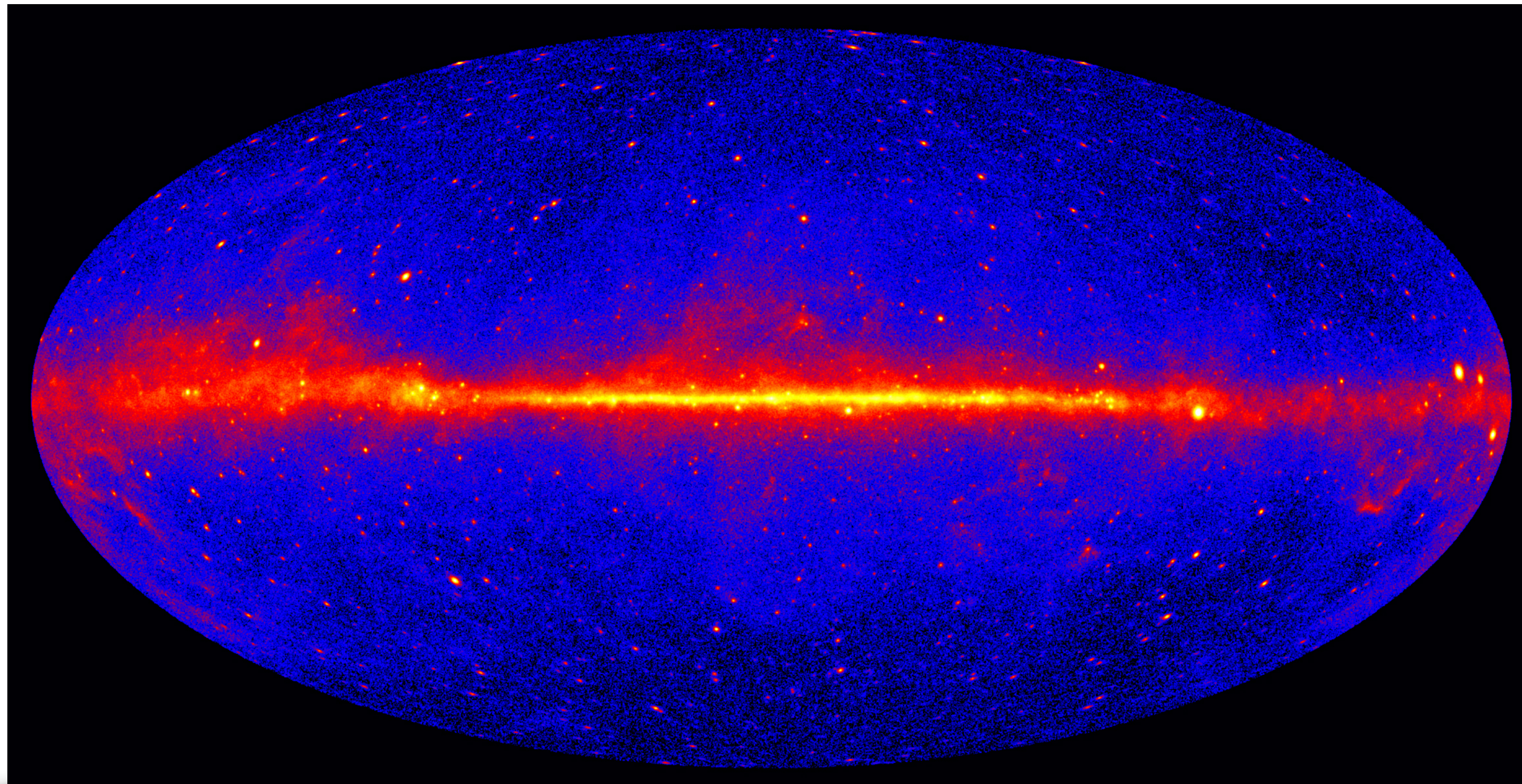
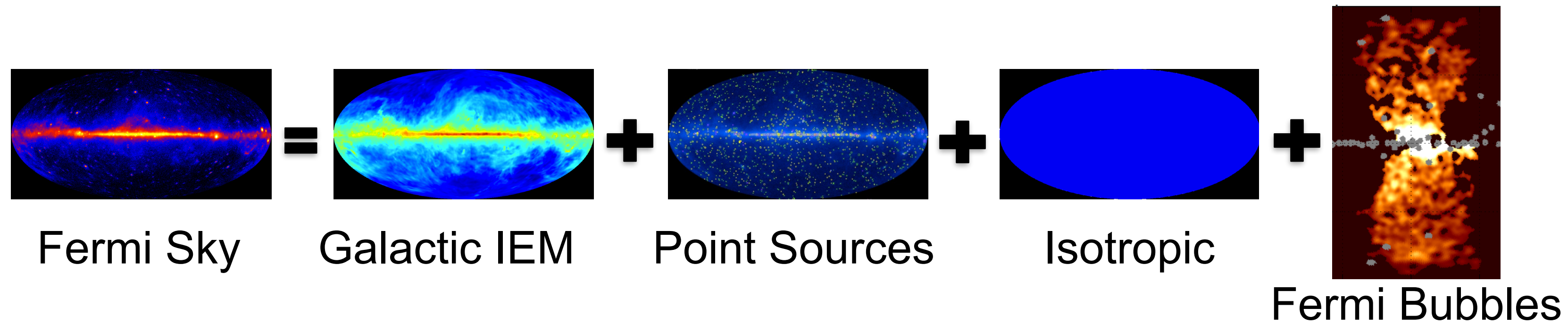
This project has received funding from the European Union's Horizon 2020 research and innovation programme under the Marie Skłodowska-Curie grant agreement No 754496

Gamma-ray map from dark matter annihilation

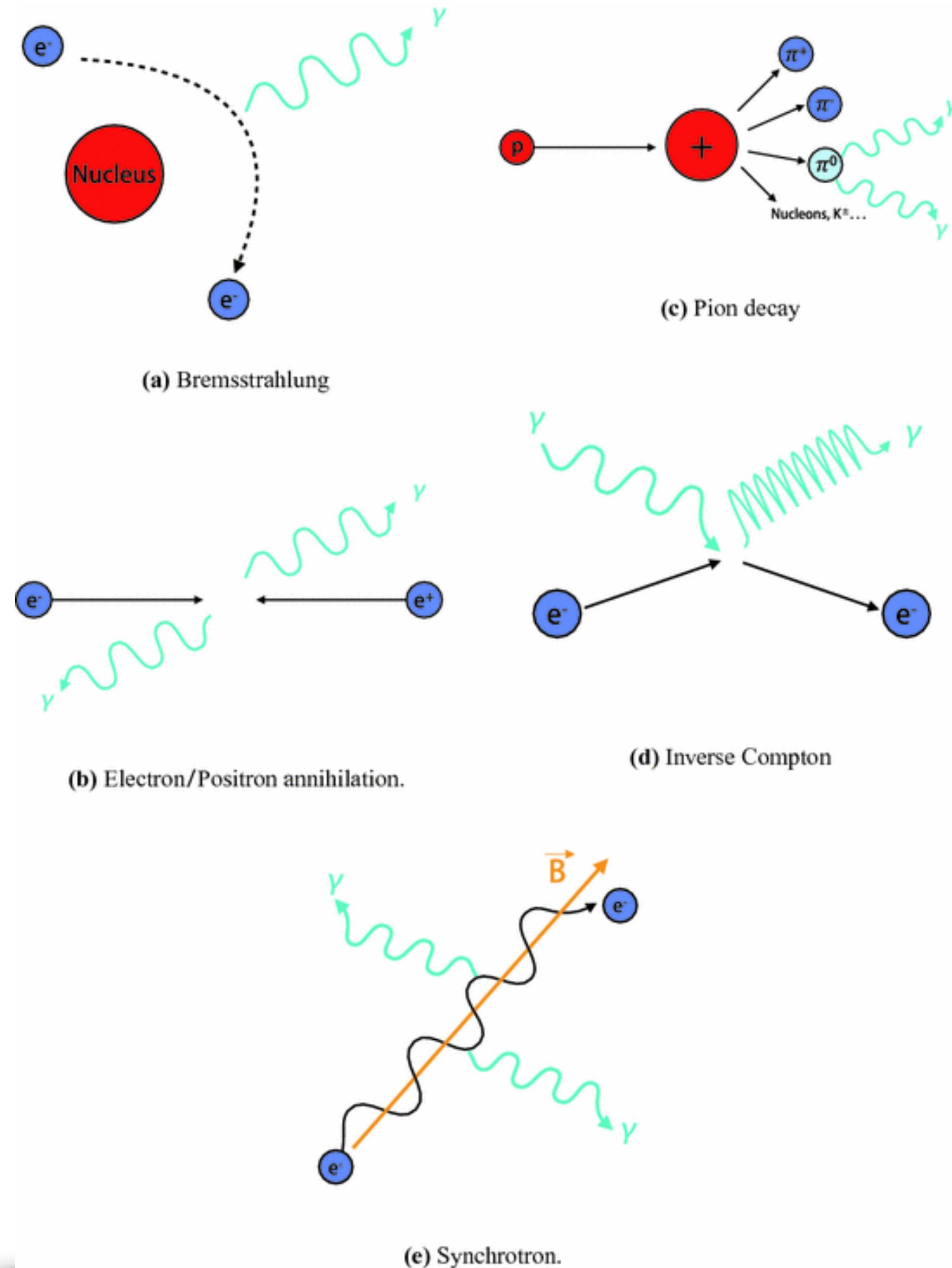


Dark Matter simulation: Pieri+
[2011PhRvD..83b3518P](#)

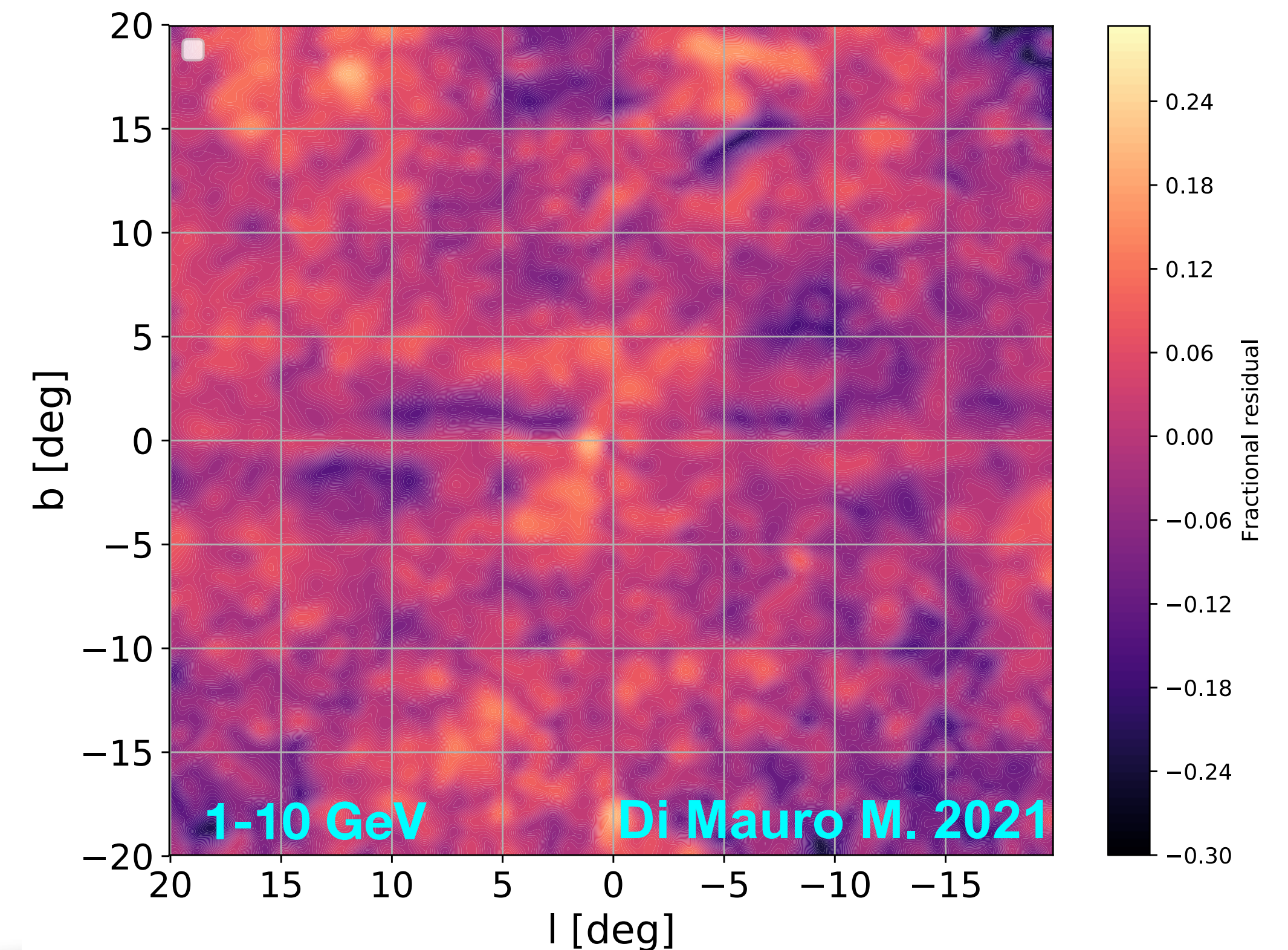
Standard picture for the gamma-ray sky



Galactic interstellar emission



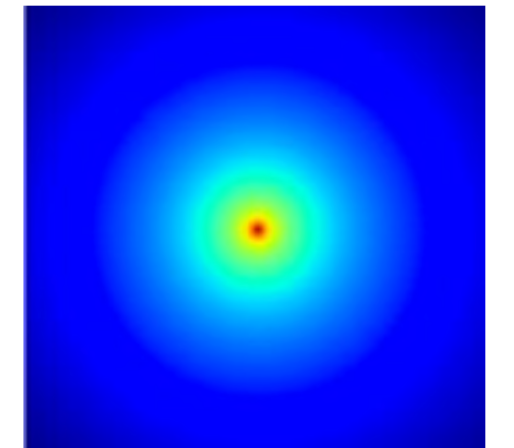
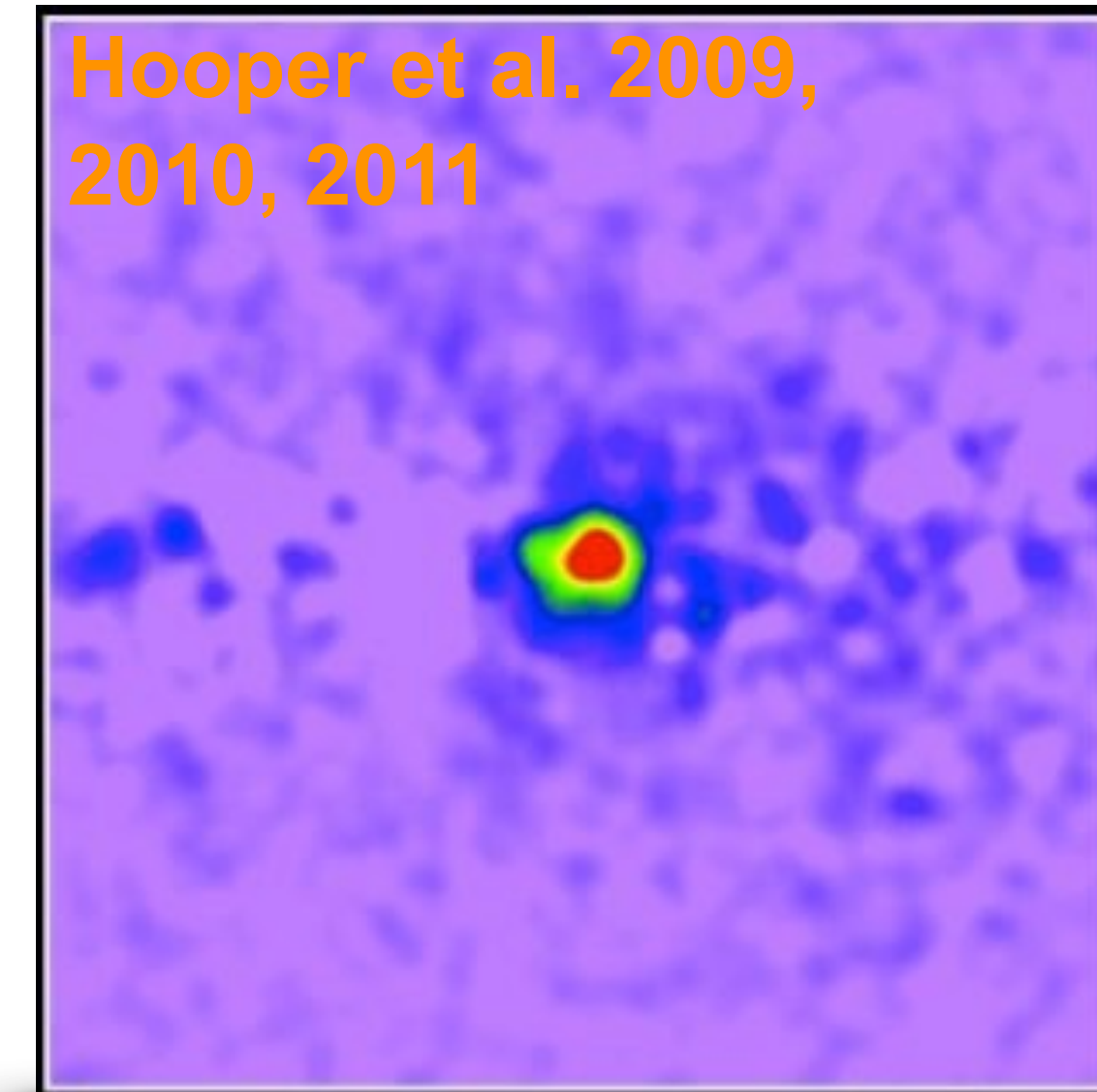
- The models usually used are divided into:
 - Bremsstrahlung, π^0 , ICS, isotropic component, Sun/Moon/Loop I and the Fermi bubbles.
- The residuals are roughly at the level of 20-25% of the data.



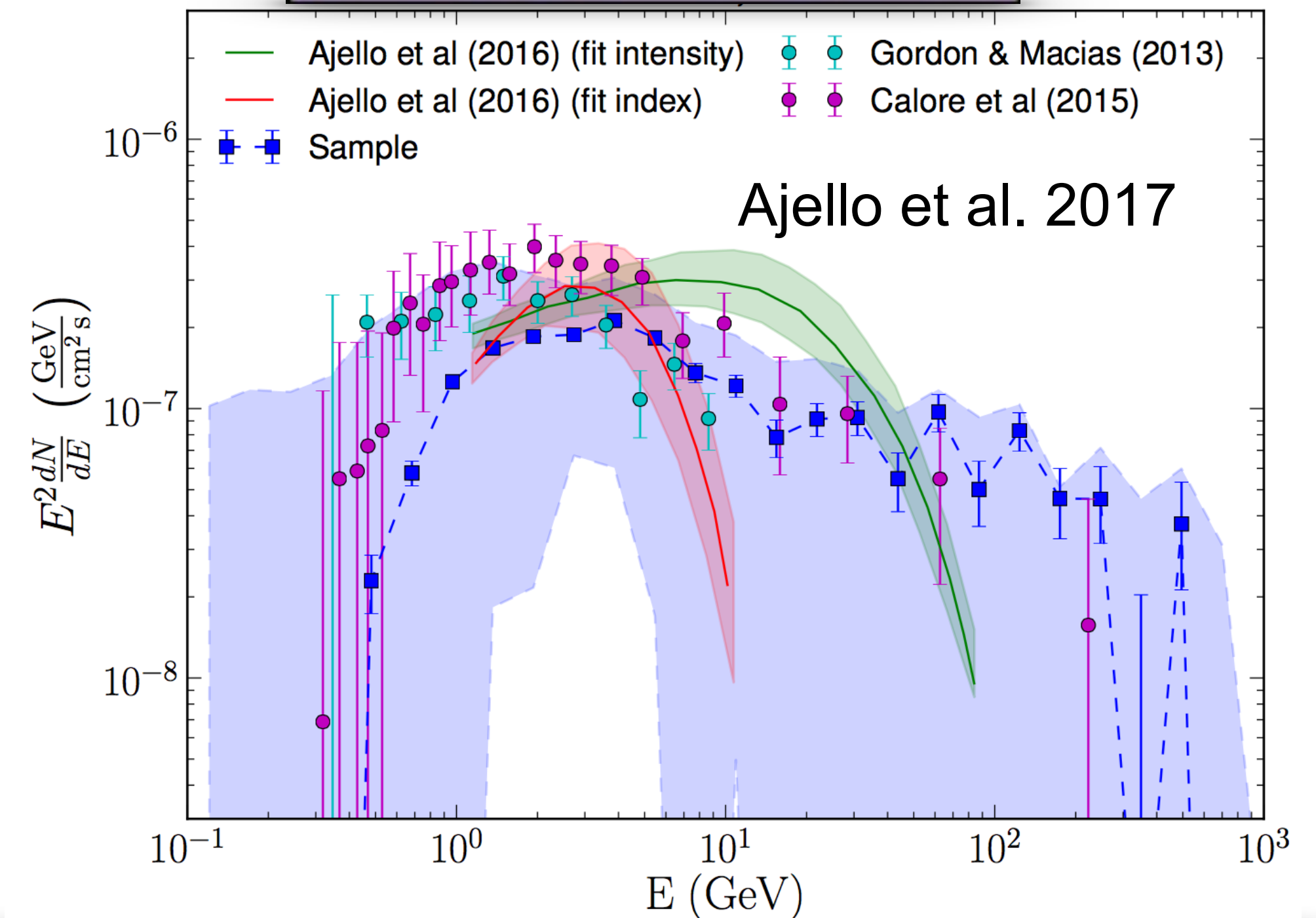
The GeV Excess in the Galactic Center (GCE)

- **Bright** and highly significant.
- **Spatially symmetric** around the Galactic center: $dN/dV \propto r^{-2.5} \rightarrow$ compatible with a gNFW profile.
- **Energy spectrum peaked at a few GeV** \rightarrow DM annihilating into a bottom-anti-bottom ($b\bar{b}$) $M_{\text{DM}}=40$ GeV.
- **Annihilation cross** section roughly equal to the thermal cross section is needed.

The GeV excess is thus perfectly compatible with DM in the halo of our Galaxy



DM



Other interpretations for the GeV excess

- Recent outbursts of CR protons or of CR leptons.
- **Hadronic scenario:** γ -ray signal extended along the Galactic plane (Petrovic et al. 2014).
- **Leptonic outburst:** correct spatial distribution but it requires at least two outbursts (Petrovic et al. 2014; Carlson et al. 2014; Cholis et al. 2015a; Gaggero et al. 2015).
- **Additional population of supernova remnants near the GC** (Gaggero et al. 2015; Carlson et al. 2016).
- **Pulsars around the Galactic bulge.**
 - **Bartels et al. (2015) and Lee et al. (2015):** population of unresolved sources distributed in the Galactic bulge of our Galaxy Pulsars in the Galactic bulge (Macias et al).
 - The spatial distribution, total γ -ray emission and energy spectrum of this unresolved emission of pulsars is compatible with the GeV excess.
 - A fraction of these faint sources should be detected with future Fermi-LAT catalogs (Bartels et al. 2015 and Hooper et al. 2014).

Papers related to this talk

Investigating the *Fermi* Large Area Telescope sensitivity of detecting the characteristics of the Galactic center excess

Paper I

Mattia Di Mauro,*

PRD 102, 103013 2020

*NASA Goddard Space Flight Center, Greenbelt, MD 20771, USA and
Catholic University of America, Department of Physics, Washington DC 20064, USA*

The characteristics of the Galactic center excess measured with 11 years of *Fermi*-LAT data

Paper II

Mattia Di Mauro,*

PRD 103, 063029 (2021)

*NASA Goddard Space Flight Center, Greenbelt, MD 20771, USA and
Catholic University of America, Department of Physics, Washington DC 20064, USA*

Multimessenger constraints on the dark matter interpretation of the *Fermi*-LAT Galactic center excess

Paper III

Mattia Di Mauro

PRD 103, 123005 (2021)

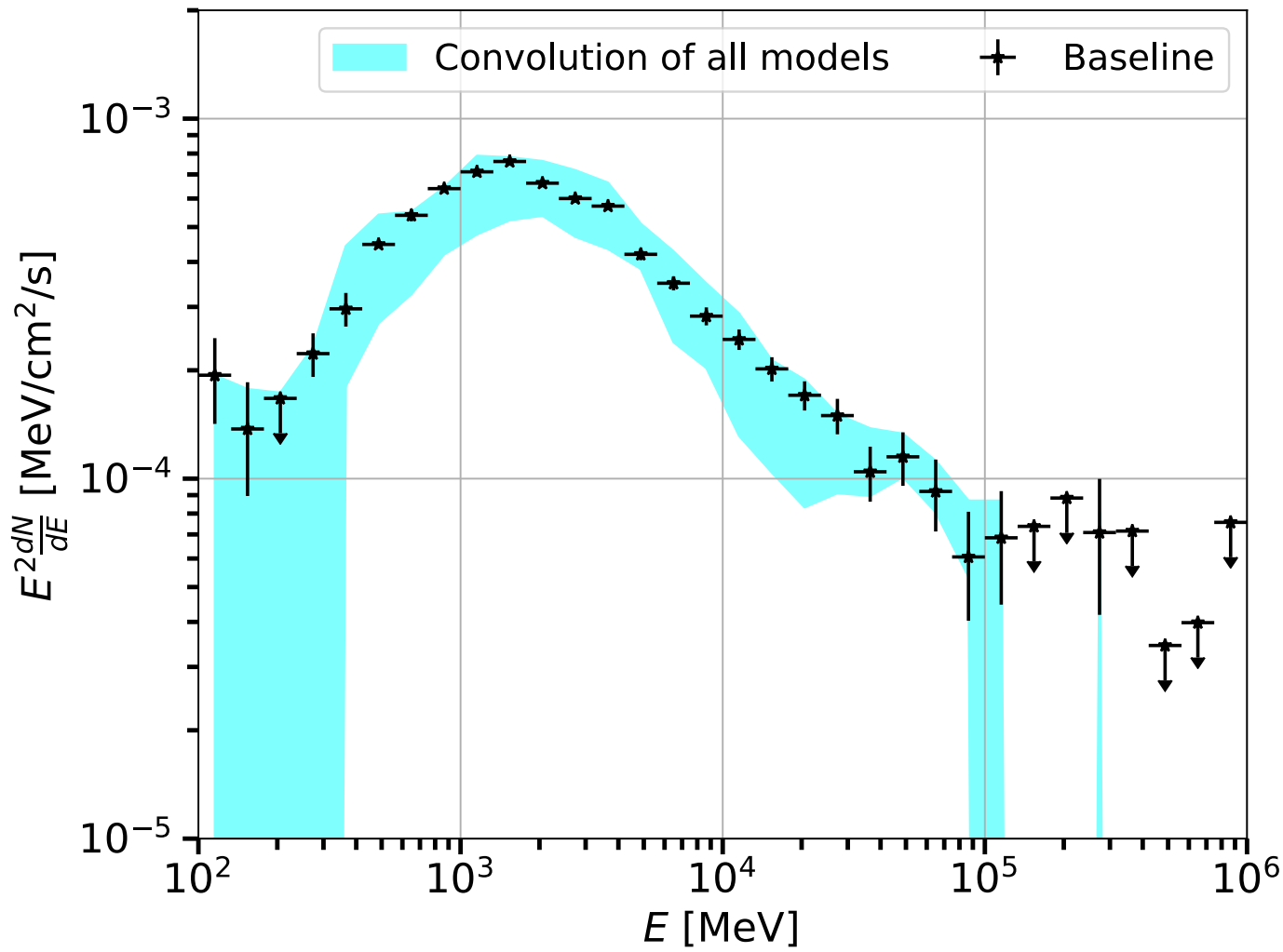
Istituto Nazionale di Fisica Nucleare, via P. Giuria, 1, 10125 Torino, Italy

Martin Wolfgang Winkler

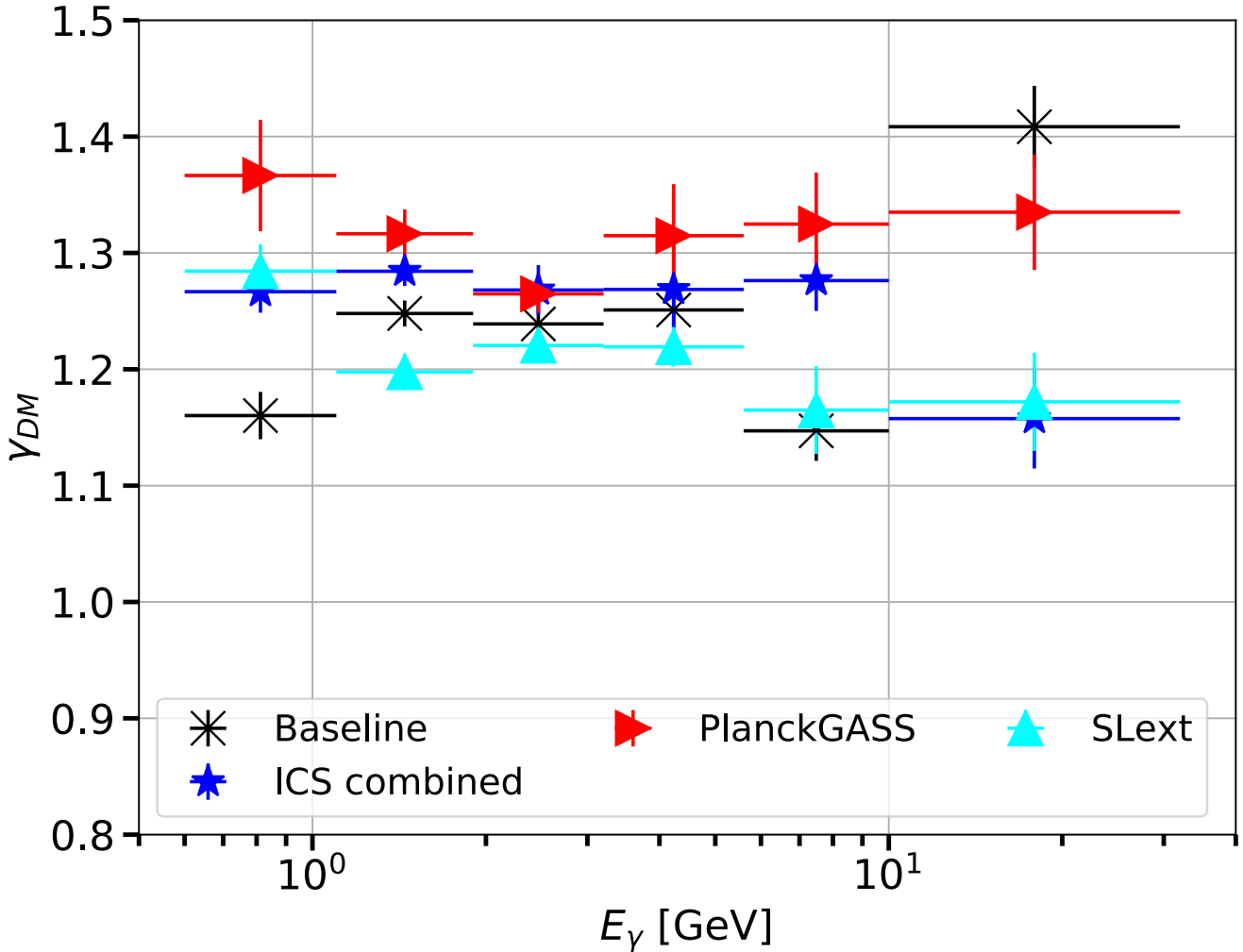
Stockholm University and The Oskar Klein Centre for Cosmoparticle Physics, Alba Nova, 10691 Stockholm, Sweden

Characteristics of the GCE: Summary

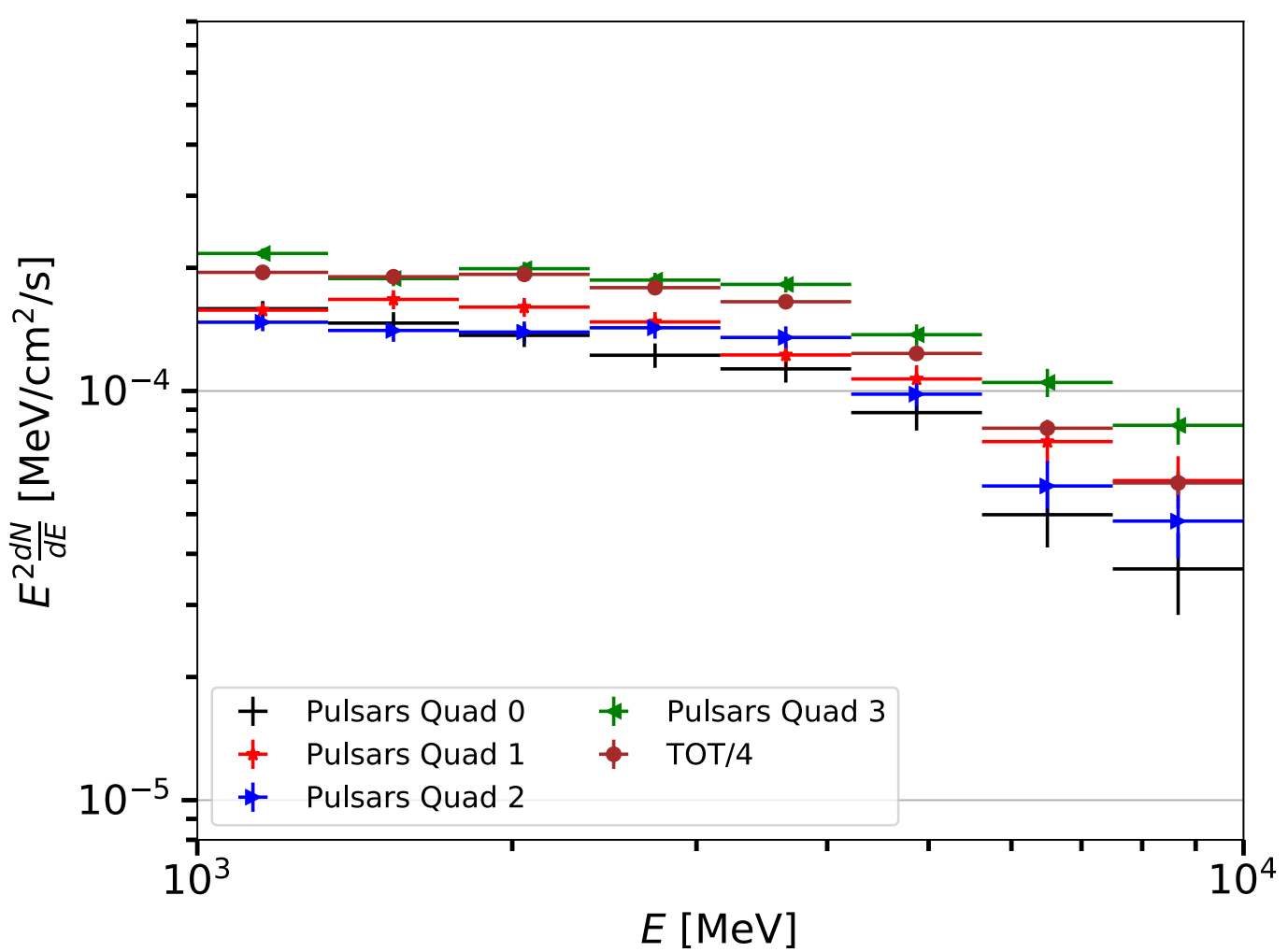
Spectrum peaked at a few GeV



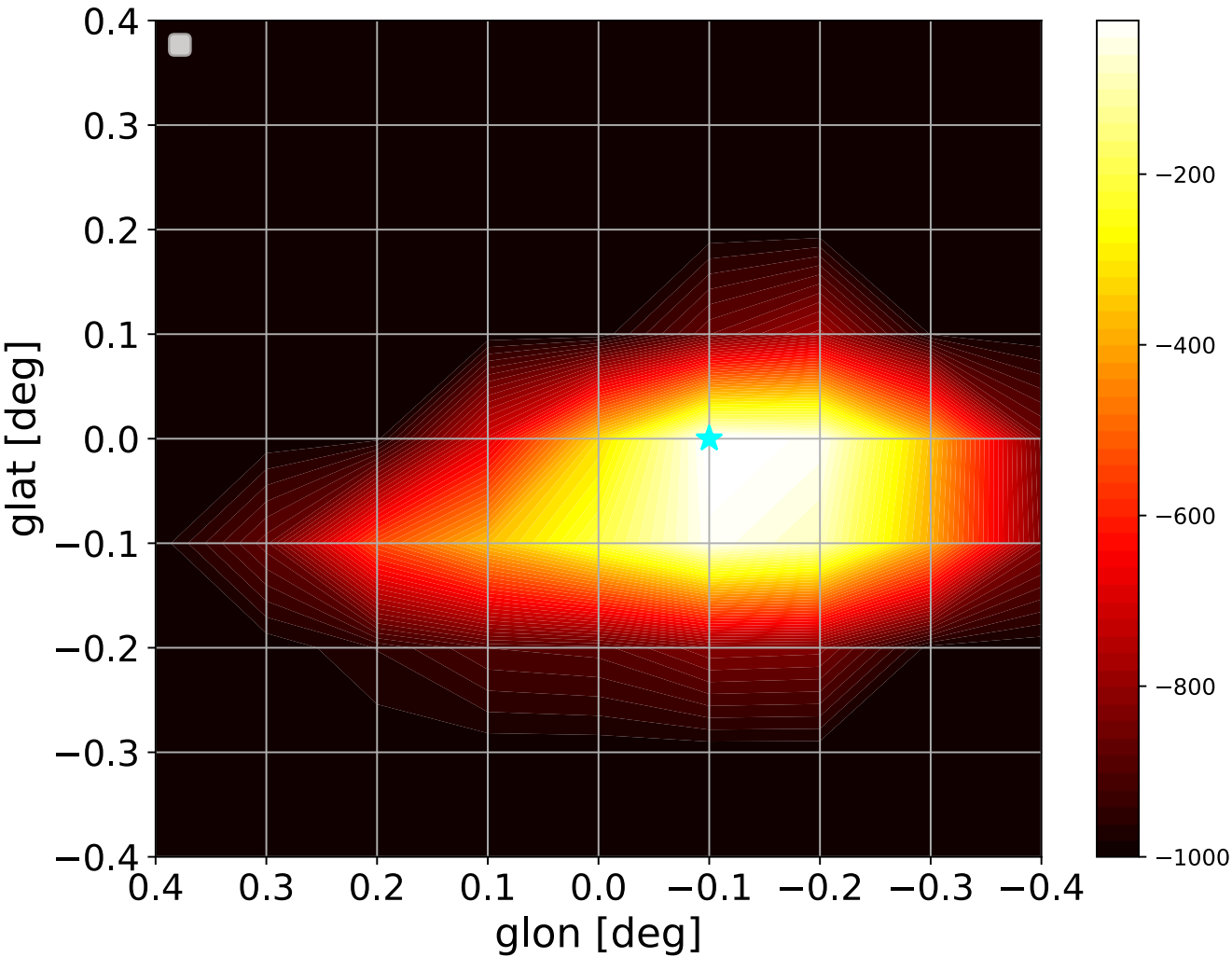
No energy dependence of spatial morphology.



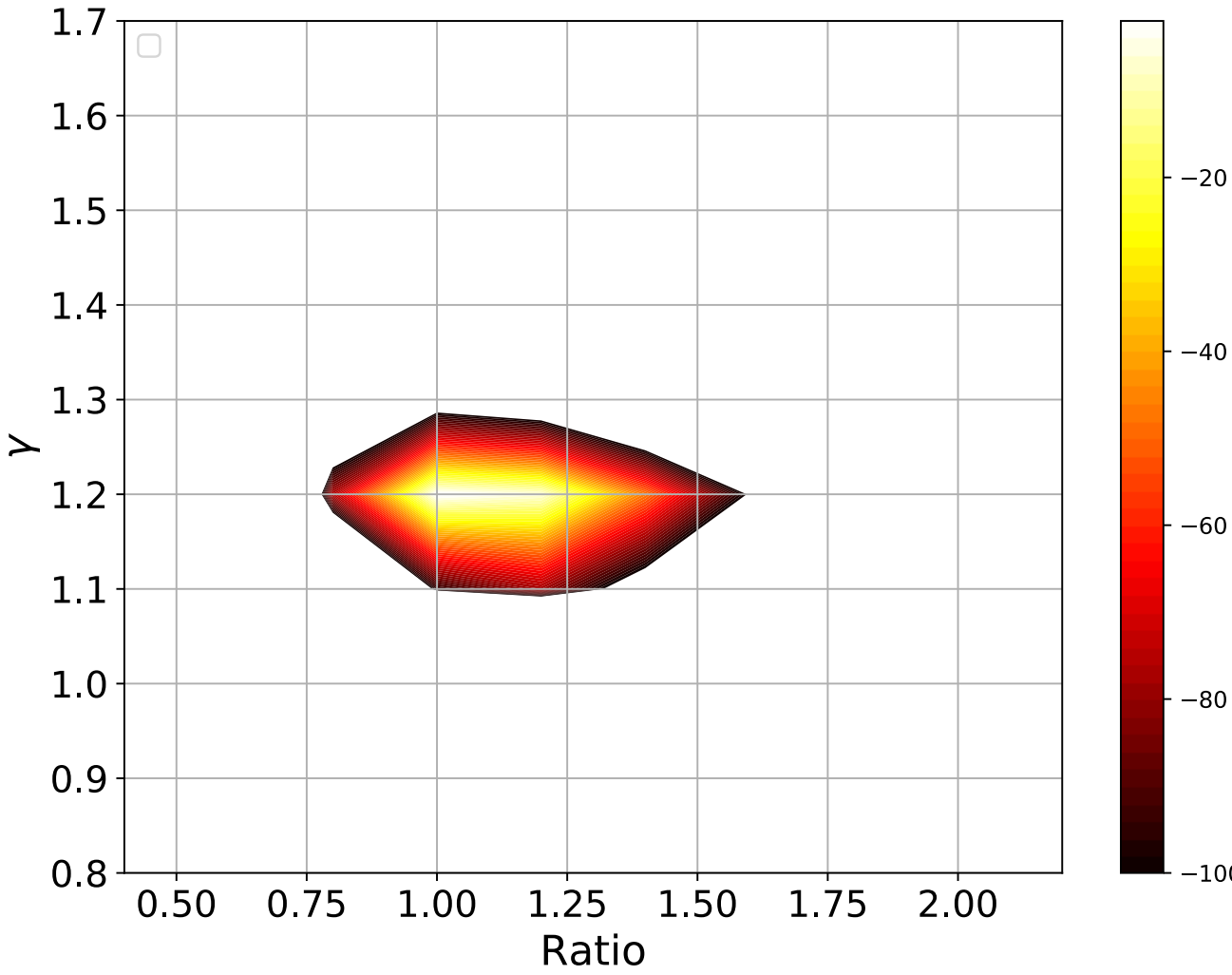
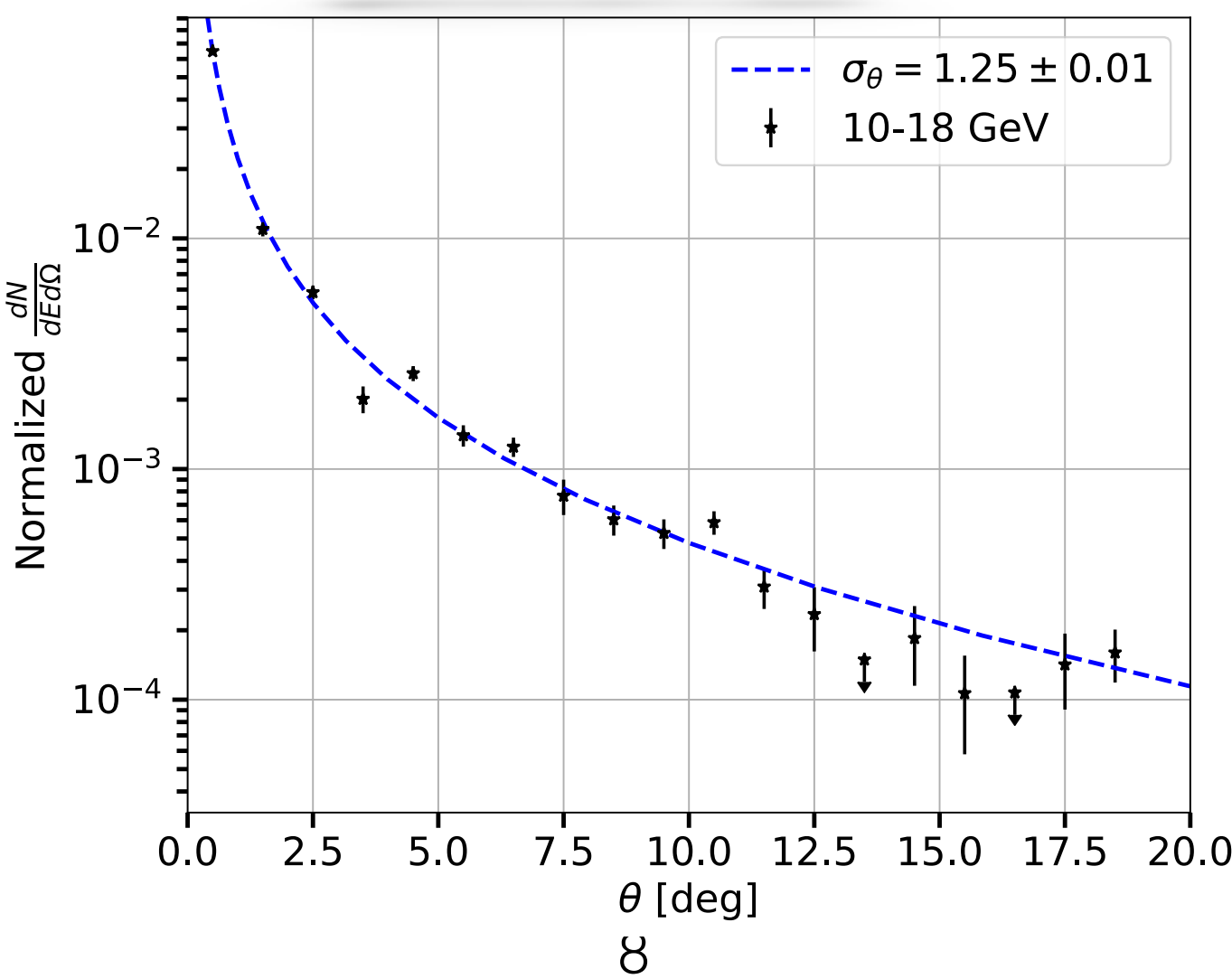
The GCE is approximatively spherically symmetric.



Centered in the GC



gamma=1.25



Dark matter density distribution

Salas et al. 2019 Rotation
curve galaxy data

DM density	slope	ρ_s [GeV/cm ³]	r_s [kpc]	\mathcal{J}
$\rho_\odot = 0.30$ GeV/cm ³ $M_{200} = 5.5 \cdot 10^{11} M_\odot$				
gNFW	1.20	0.416	12.87	111.5
gNFW	1.30	0.314	14.18	155.3
Einasto	0.13	0.376	7.25	288.9
$\rho_\odot = 0.34$ GeV/cm ³ $M_{200} = 6.2 \cdot 10^{11} M_\odot$				
gNFW	1.20	0.587	11.57	166.1
gNFW	1.30	0.449	12.67	231.0
Einasto	0.13	0.569	6.35	449.3
$\rho_\odot = 0.38$ GeV/cm ³ $M_{200} = 7.0 \cdot 10^{11} M_\odot$				
gNFW	1.20	0.851	10.20	246.8
gNFW	1.30	0.649	11.20	339.1
Einasto	0.13	0.864	5.51	686.7

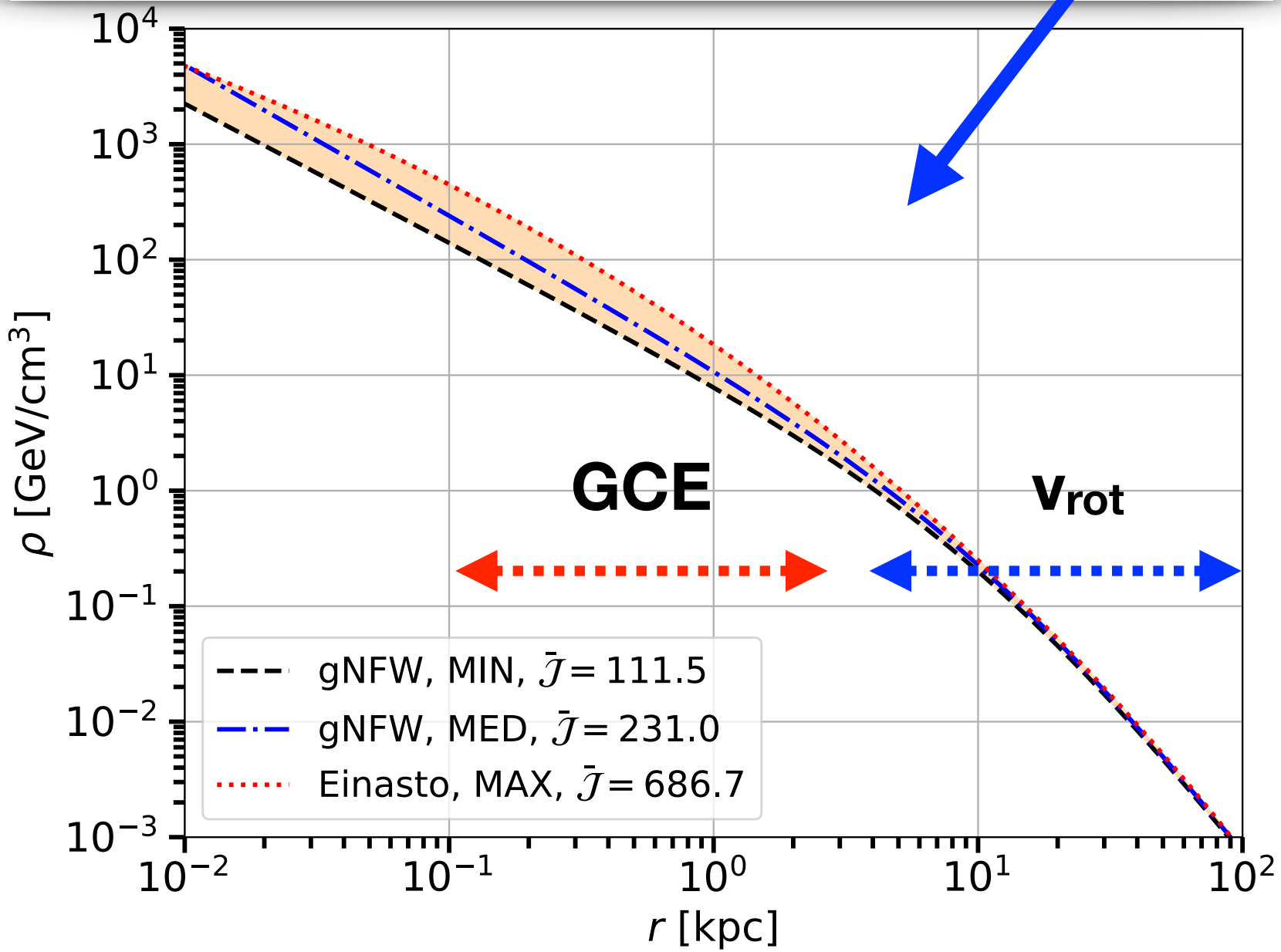
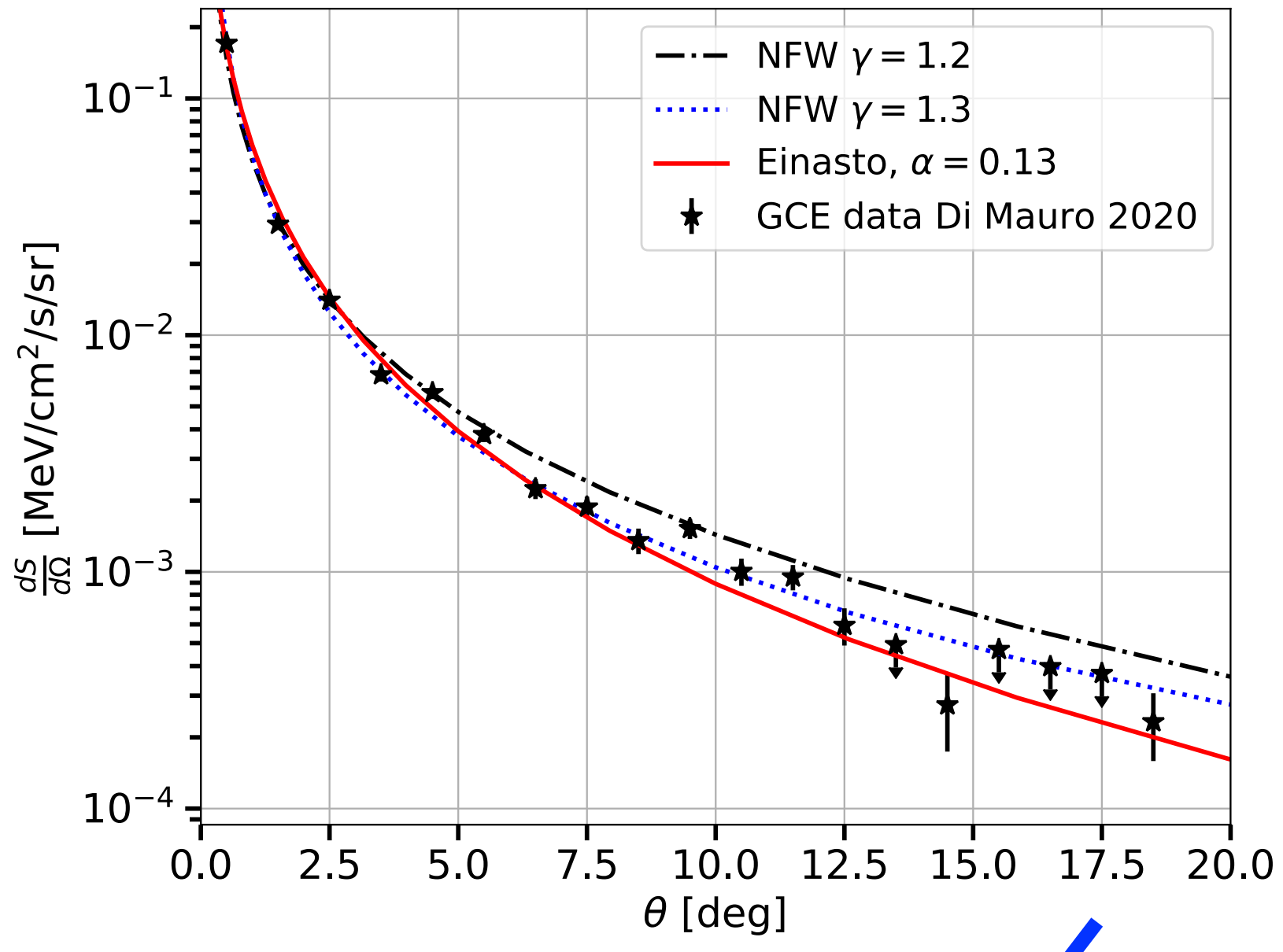
MIN

MED

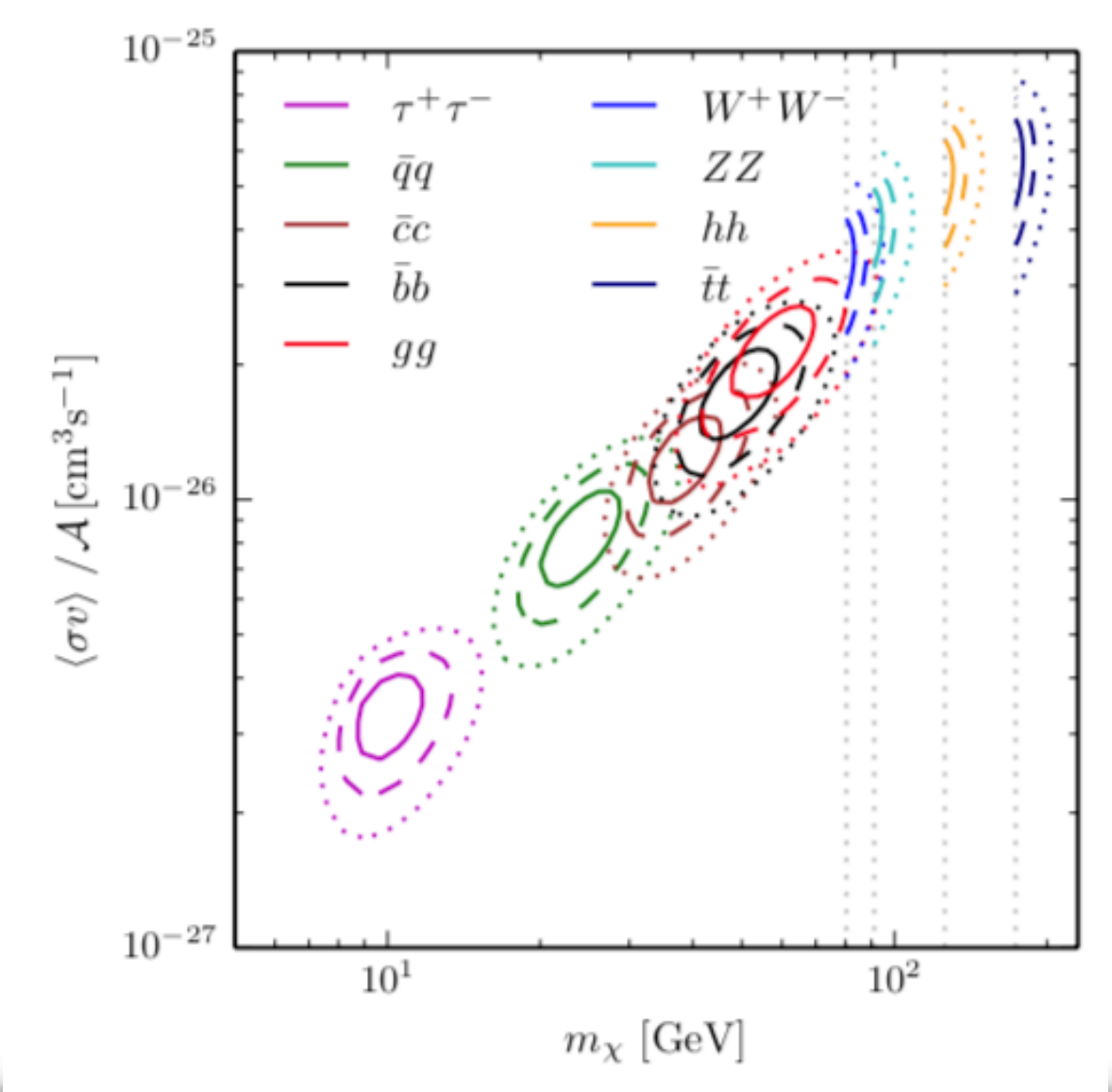
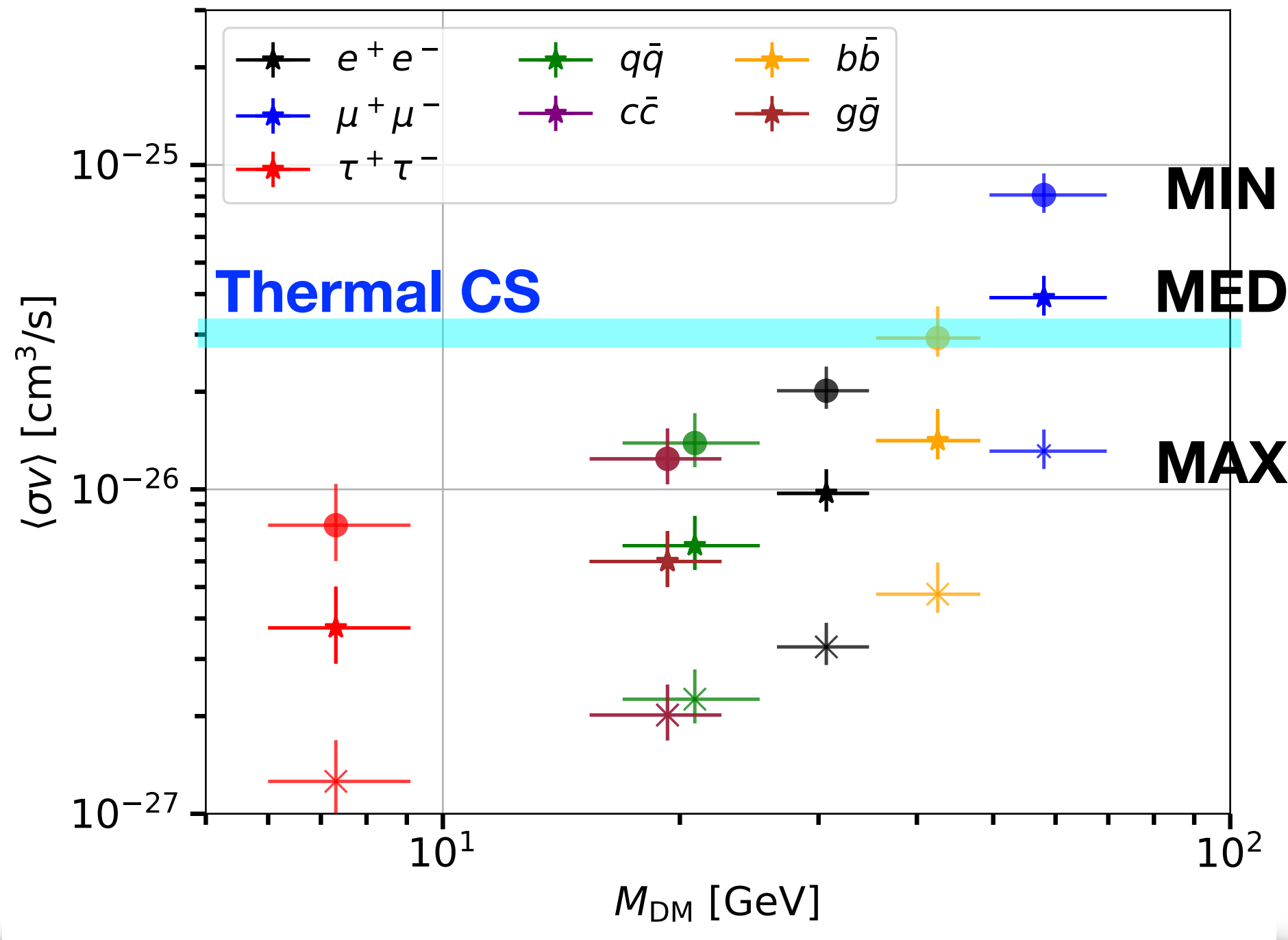
MAX

$$\bar{\mathcal{J}} = \frac{1}{\Delta\Omega} \int_{\Delta\Omega} d\Omega \int_{l.o.s.} \frac{ds}{r_\odot} \left(\frac{\rho(r(s, \Omega))}{\rho_\odot} \right)^2$$

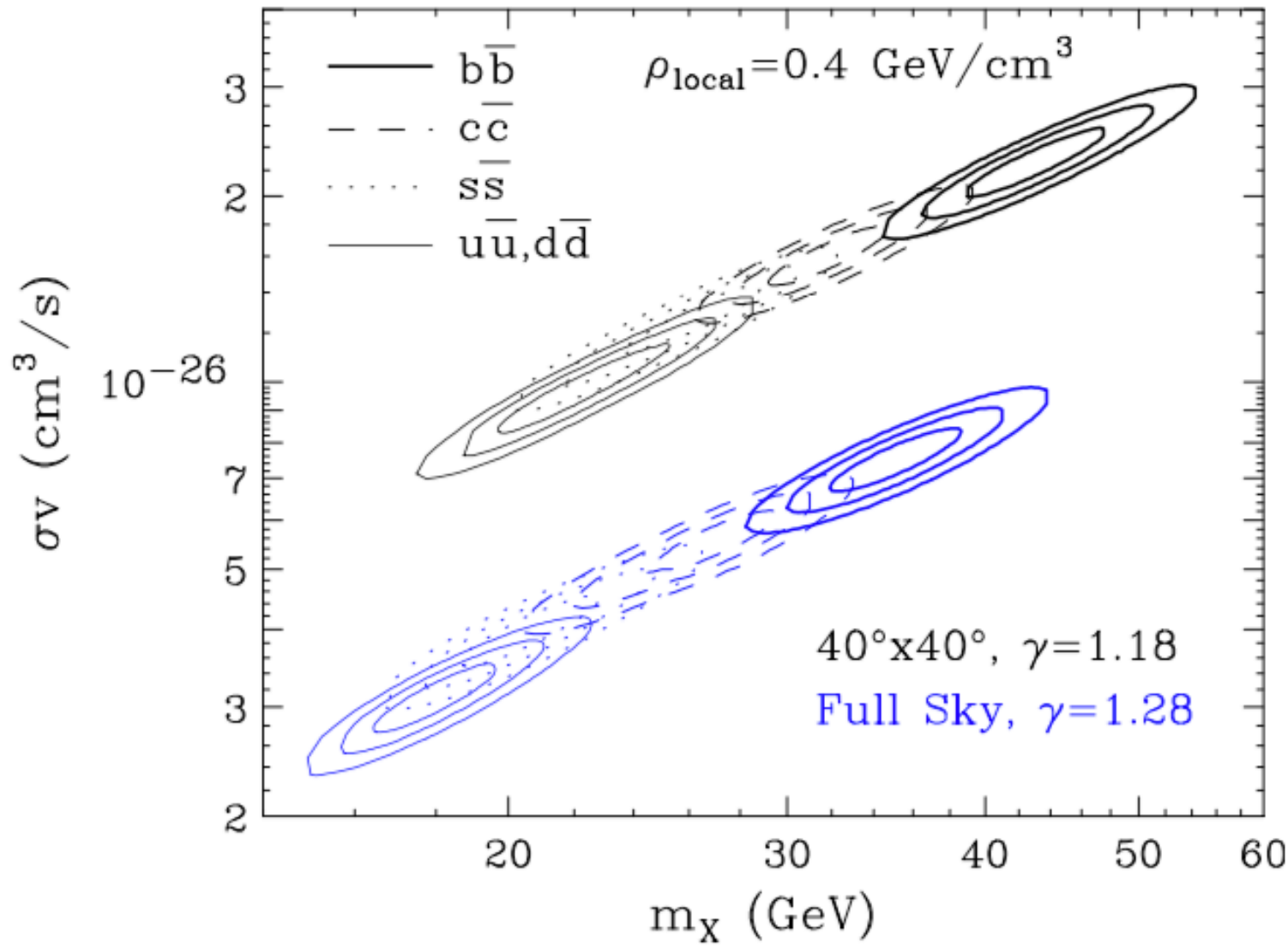
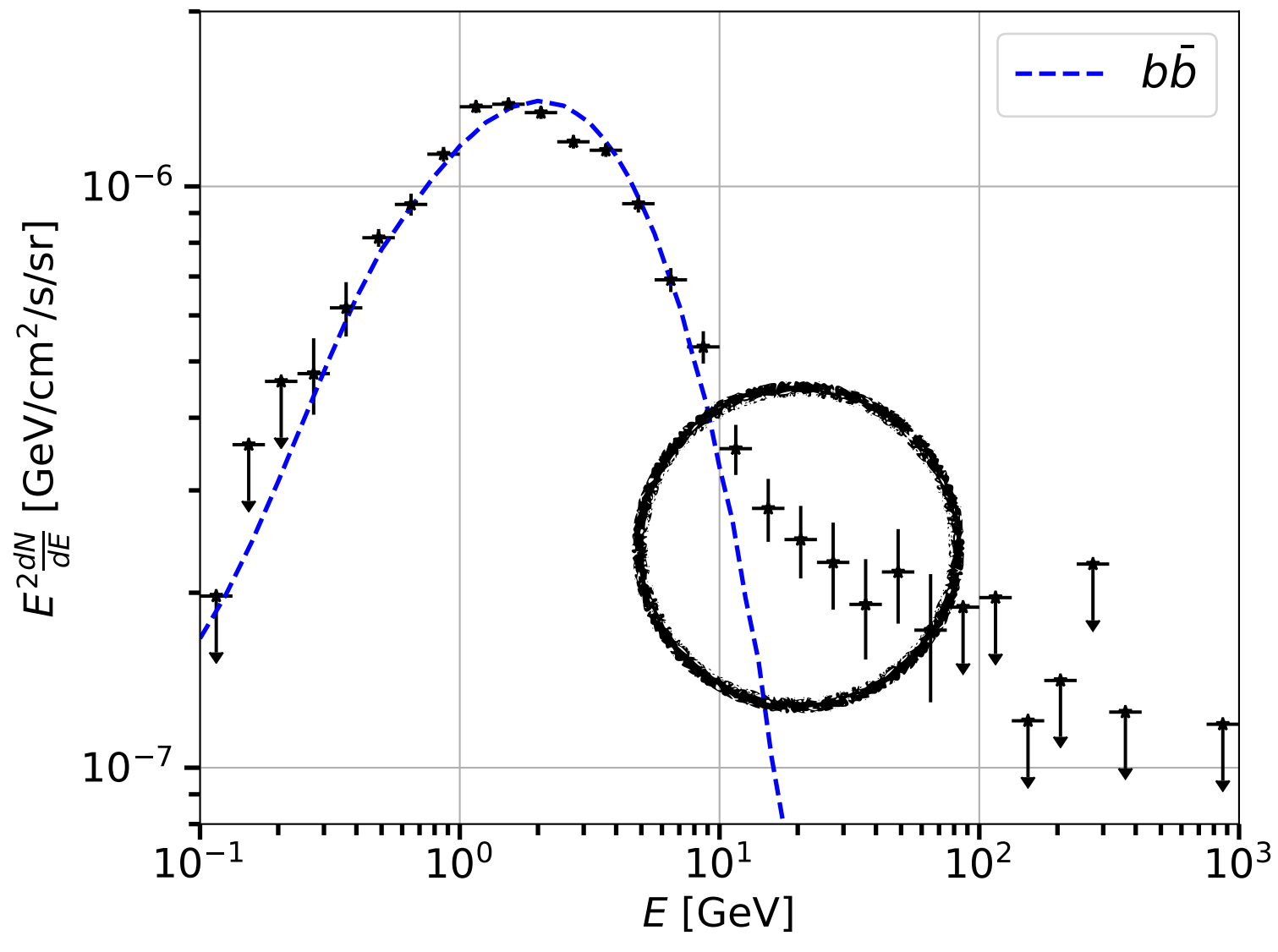
Geometrical factor integrate in our ROI



Fitting the GCE data with one channel (BR=1)



Calore et al. 2015

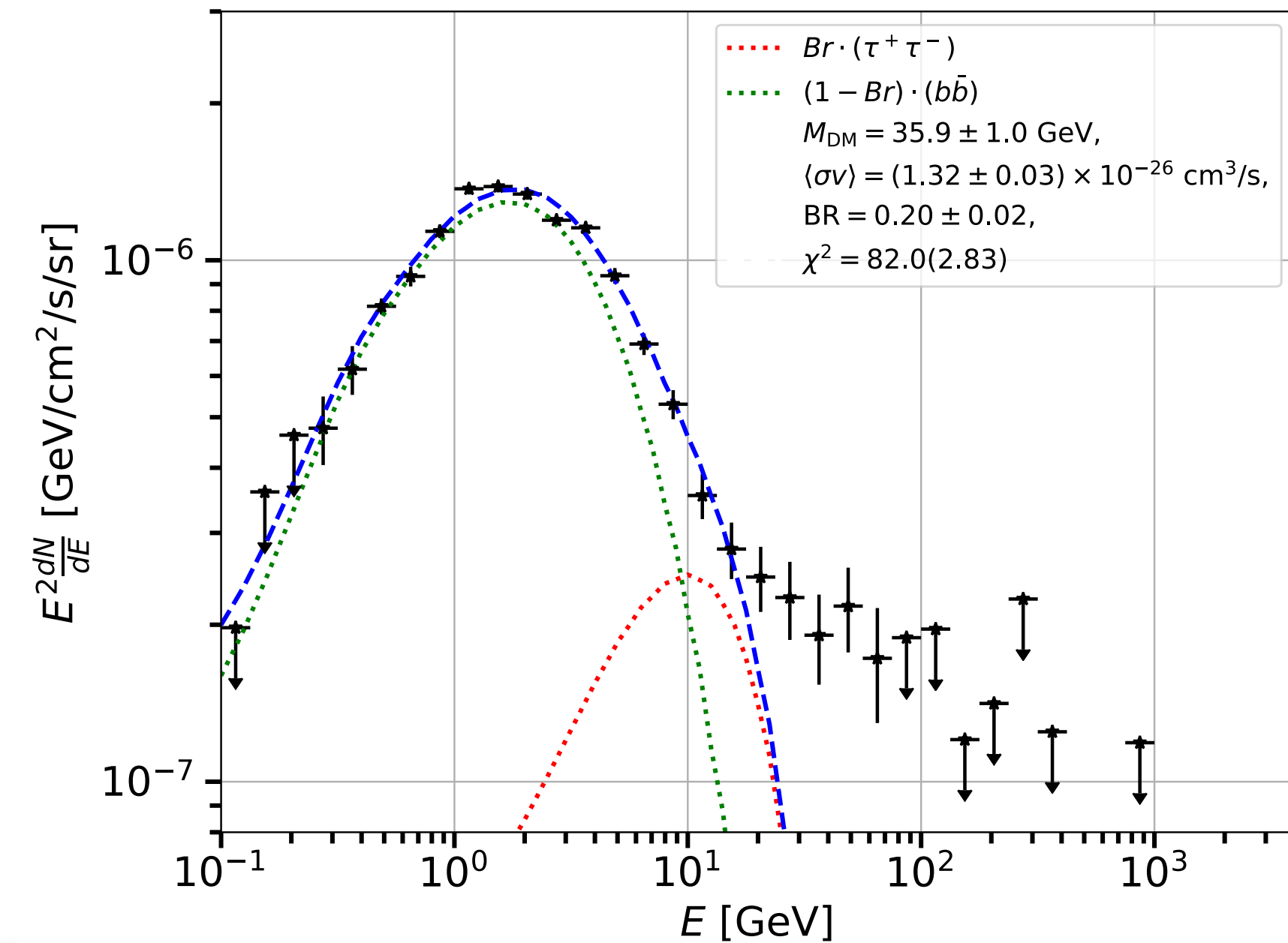
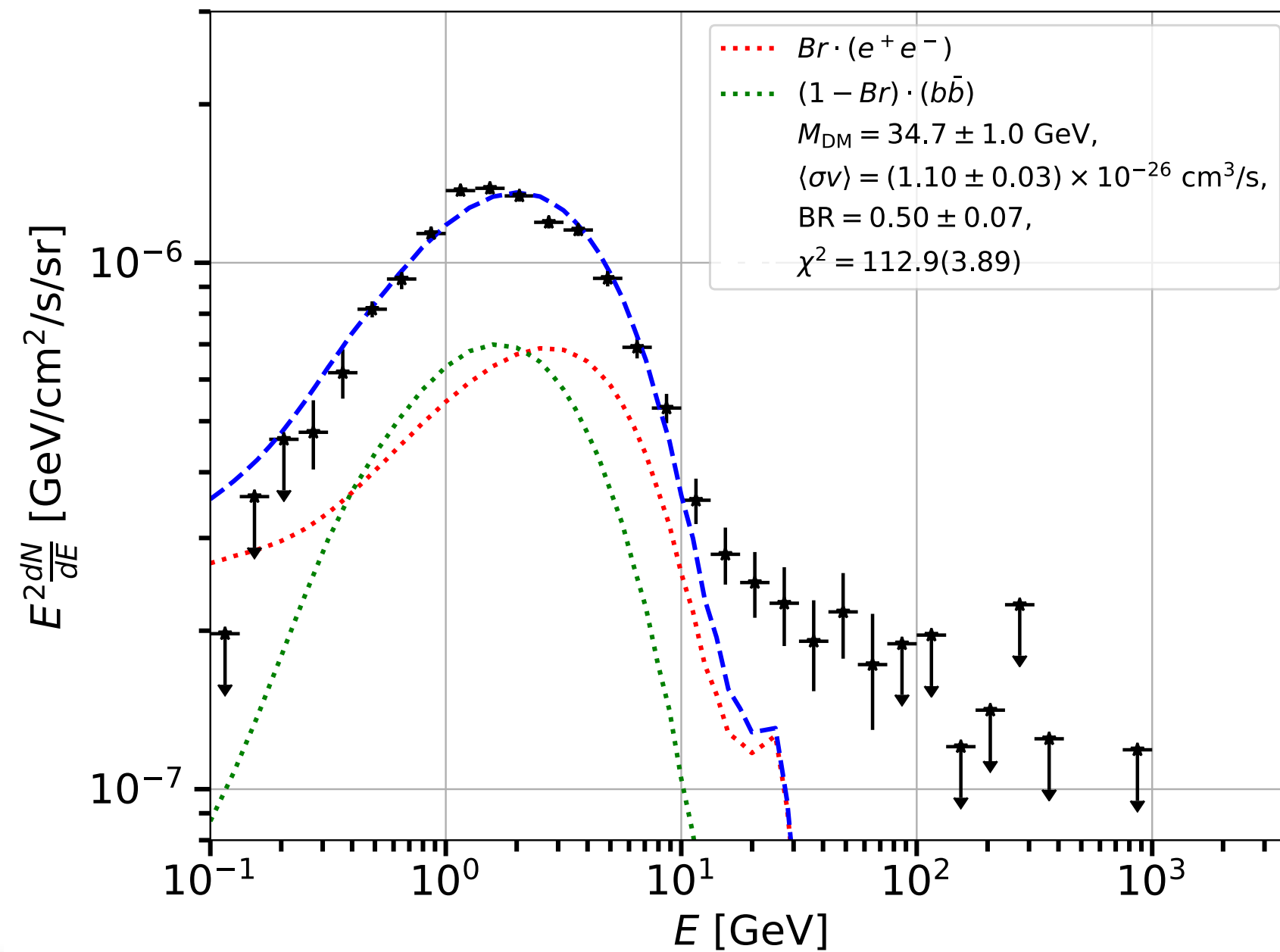


Linden et al. 2014

Fitting the GCE data with two channels

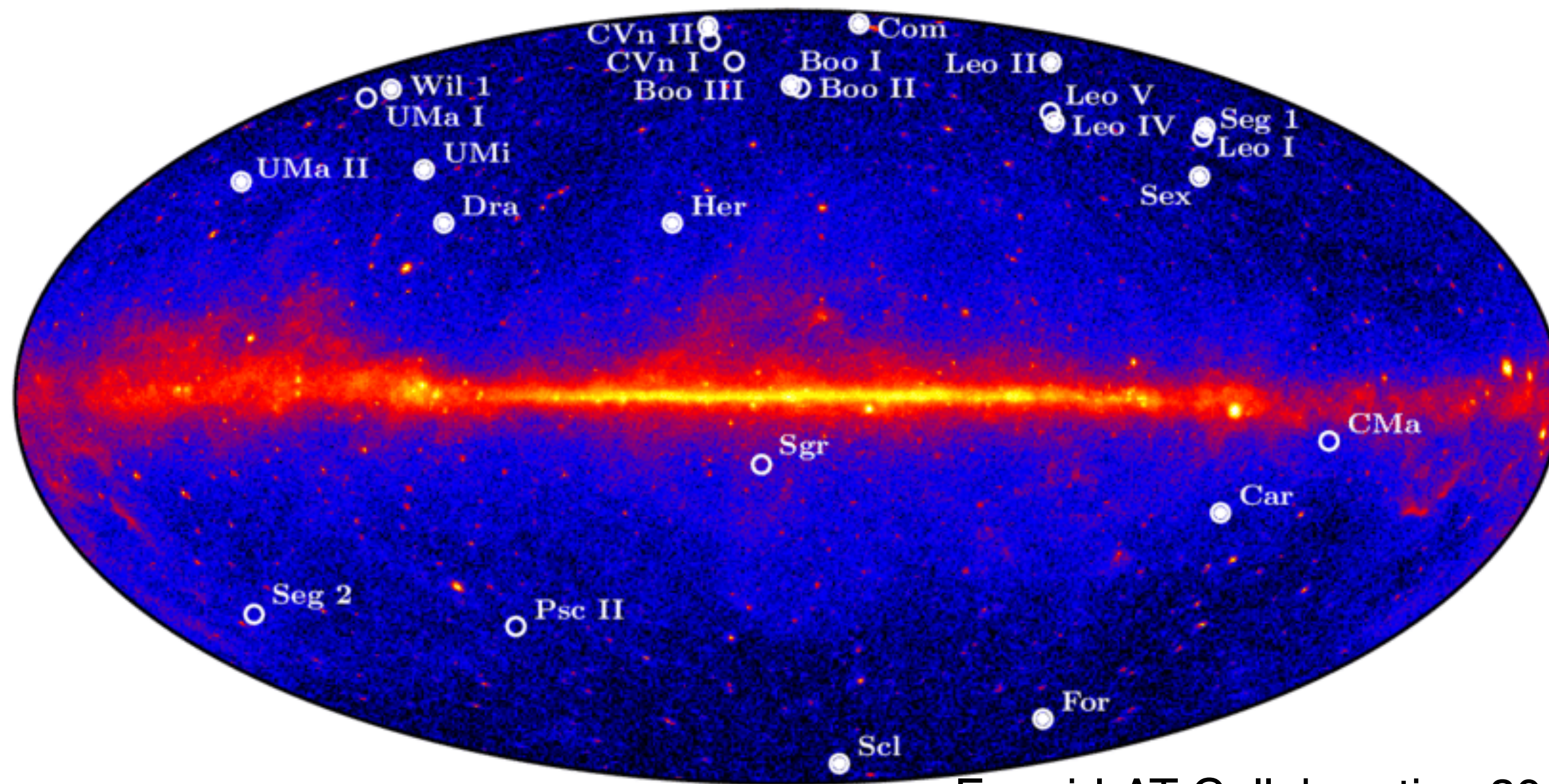
Channel 1	Channel 2	M_{DM}	$\langle\sigma v\rangle$	Br	$\chi^2(\tilde{\chi}^2)$	$\Delta\chi^2(\text{sign.})$
		[GeV]	$[10^{-26} \text{ cm}^3/\text{s}]$			
$\tau^+\tau^-$	$b\bar{b}$	35.9	1.32	0.20	82.0(2.83)	82(9.0 σ)
$\mu^+\mu^-$	$b\bar{b}$	47.8	2.42	0.65	90.5(3.12)	74(8.4 σ)
e^+e^-	$\tau^+\tau^-$	27.1	0.95	0.84	113.7(3.92)	31(5.4 σ)
e^+e^-	$c\bar{c}$	24.3	0.79	0.50	112.3(3.87)	32(5.5 σ)
e^+e^-	$b\bar{b}$	34.7	1.10	0.50	112.9(3.89)	32(5.5 σ)
$c\bar{c}$	$b\bar{b}$	33.8	1.11	0.32	115.1(3.97)	61(7.7 σ)

$$\frac{dN_\gamma}{dE} = Br \frac{dN_{\tau^+\tau^-}}{dE} + (1 - Br) \frac{dN_{b\bar{b}}}{dE}$$



Milky Way dwarf spheroidal satellite galaxies

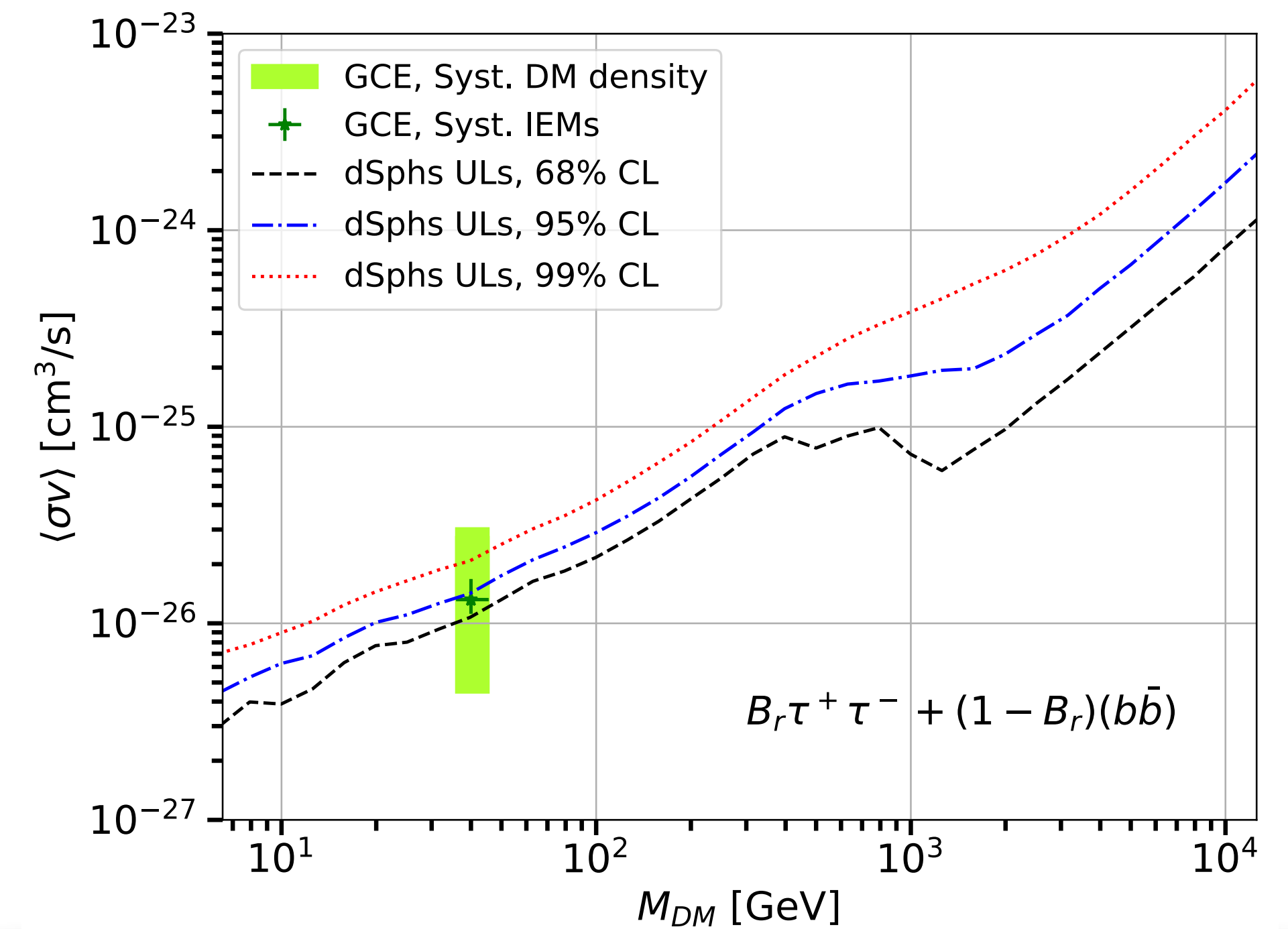
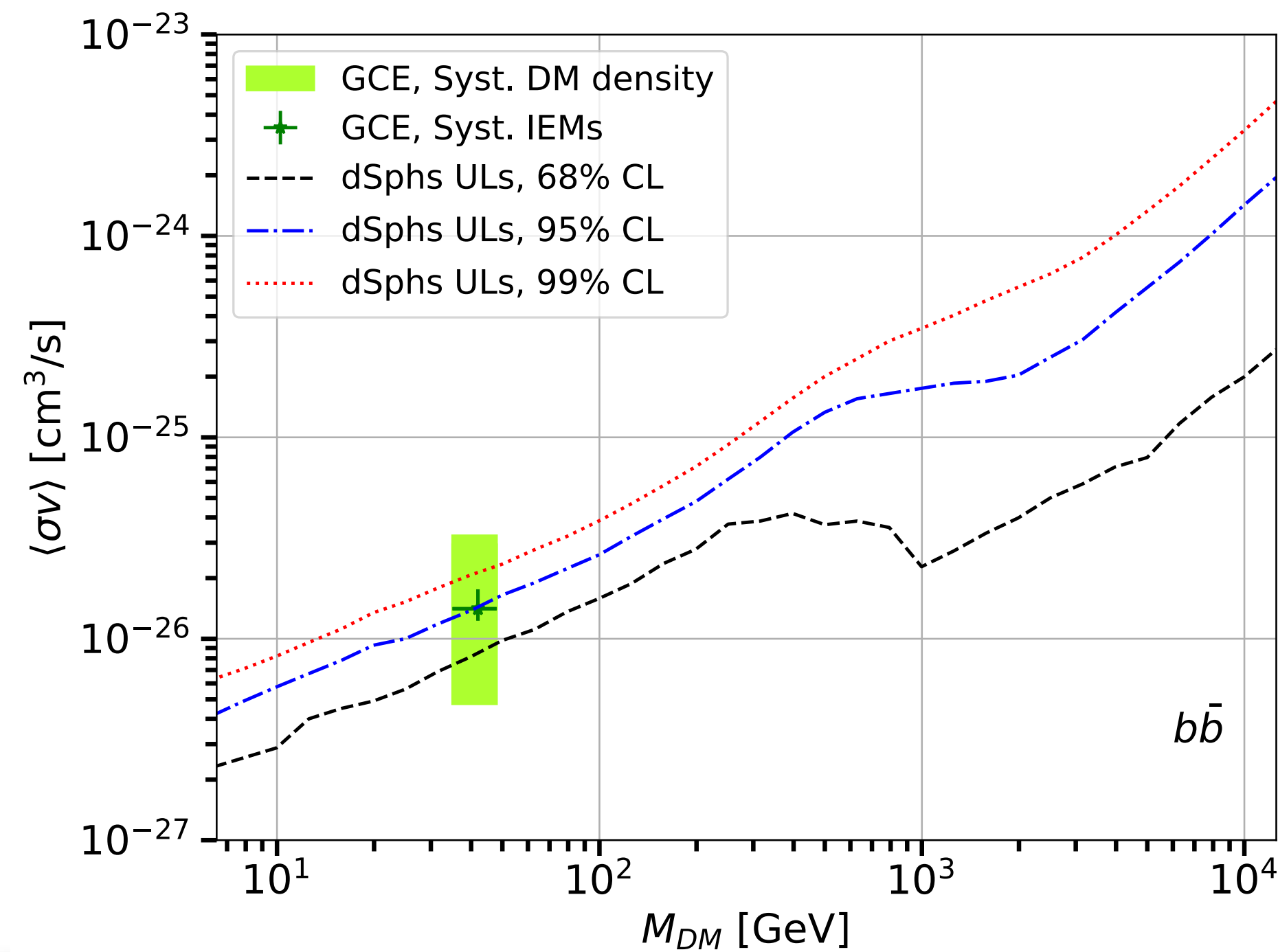
- dSphs are among the most promising targets for the indirect search of DM with γ -rays.
- Mass-to-luminosity ratio of the order of 100 – 1000.
- They have an environment with predicted low astrophysical background



Fermi-LAT Collaboration 2013

Combined analysis for dSphs

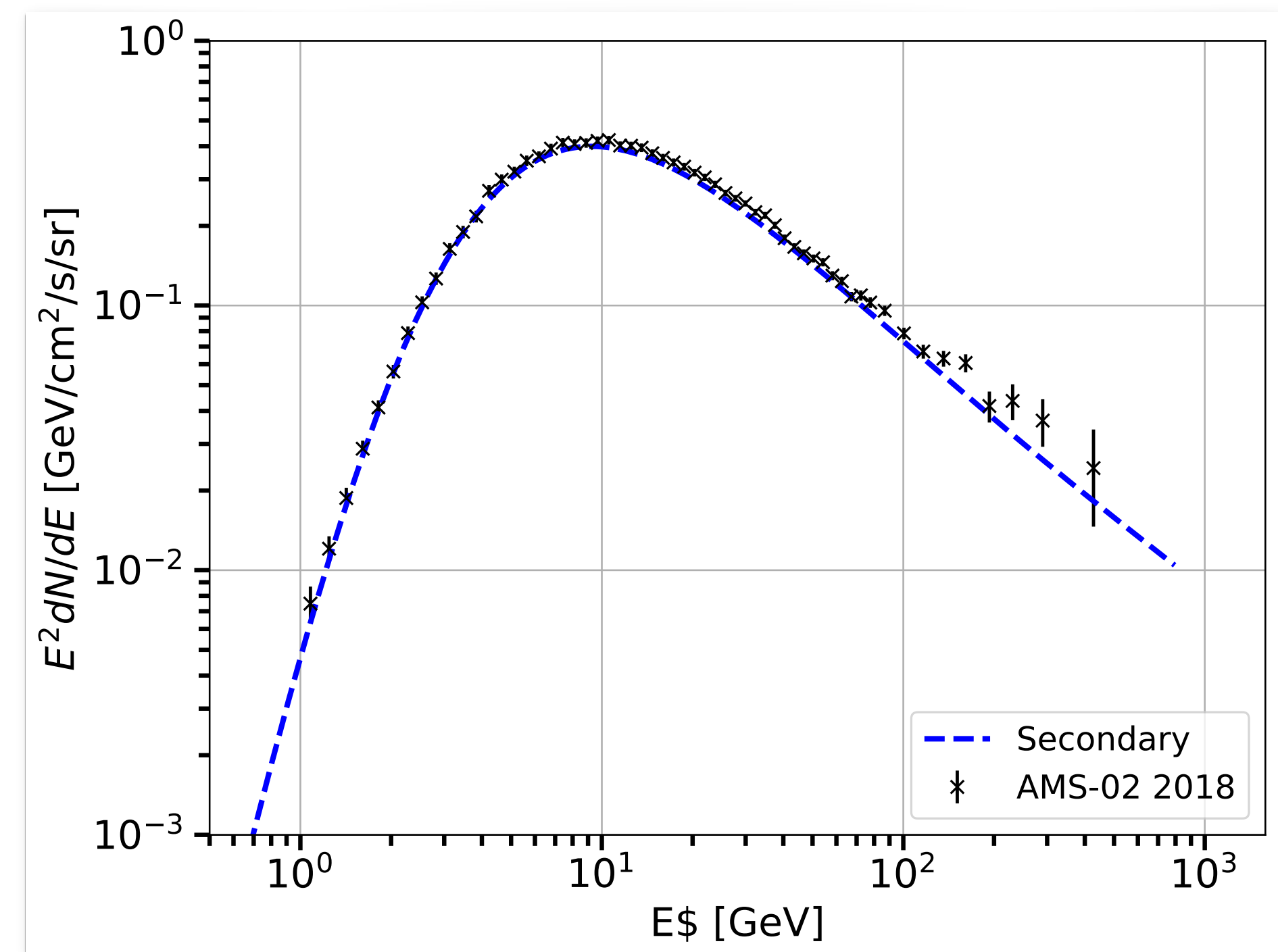
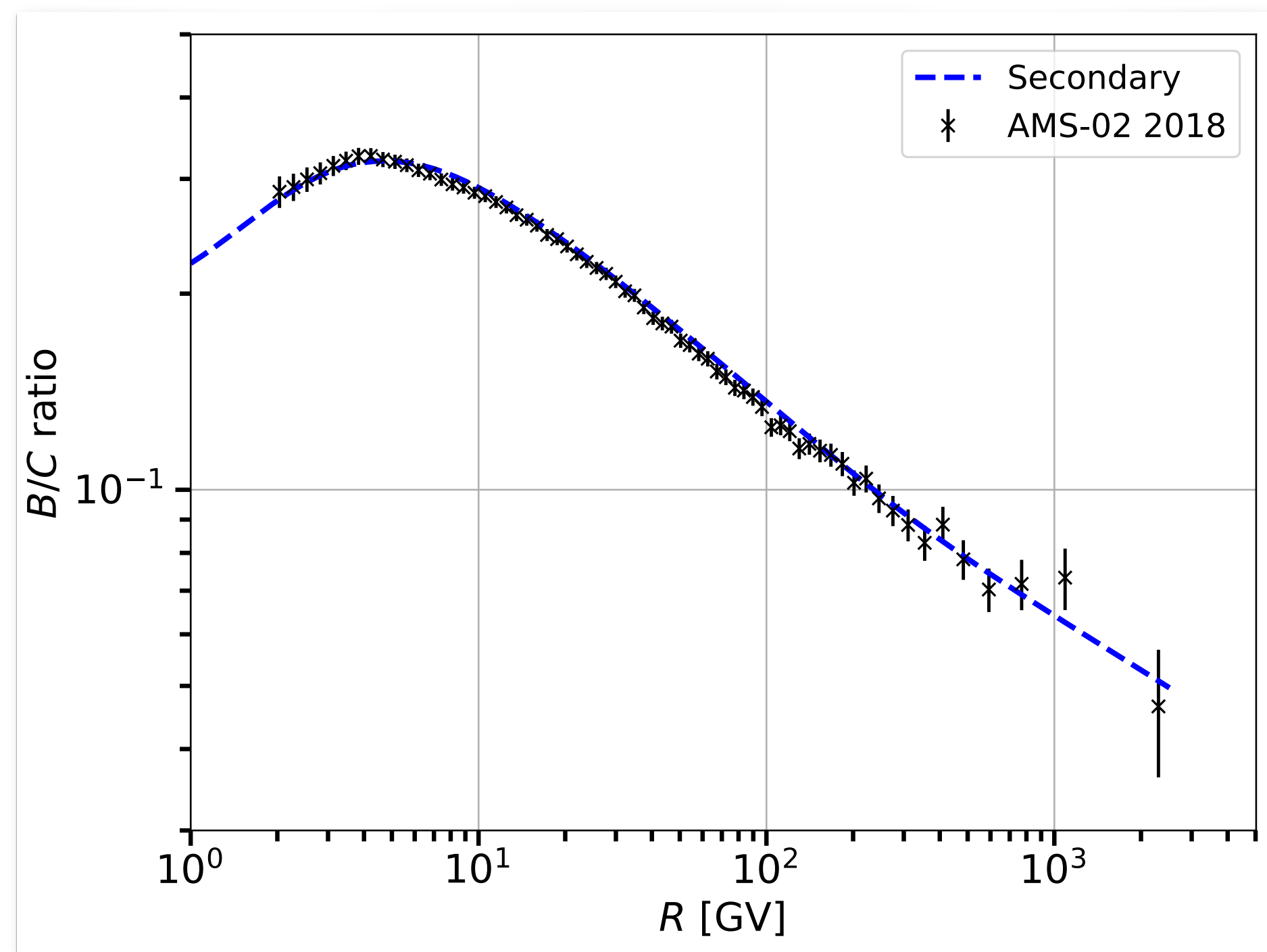
- We perform a combined analysis of 48 dSphs (Pace and Strigari 2018).
 - We also test the sample from Albert et al. 2017.
- The pipeline we use is the one employed in previous *Fermi*-LAT papers.
- There is no significant emission in the stacked sample.



Antiprotons vs GCE

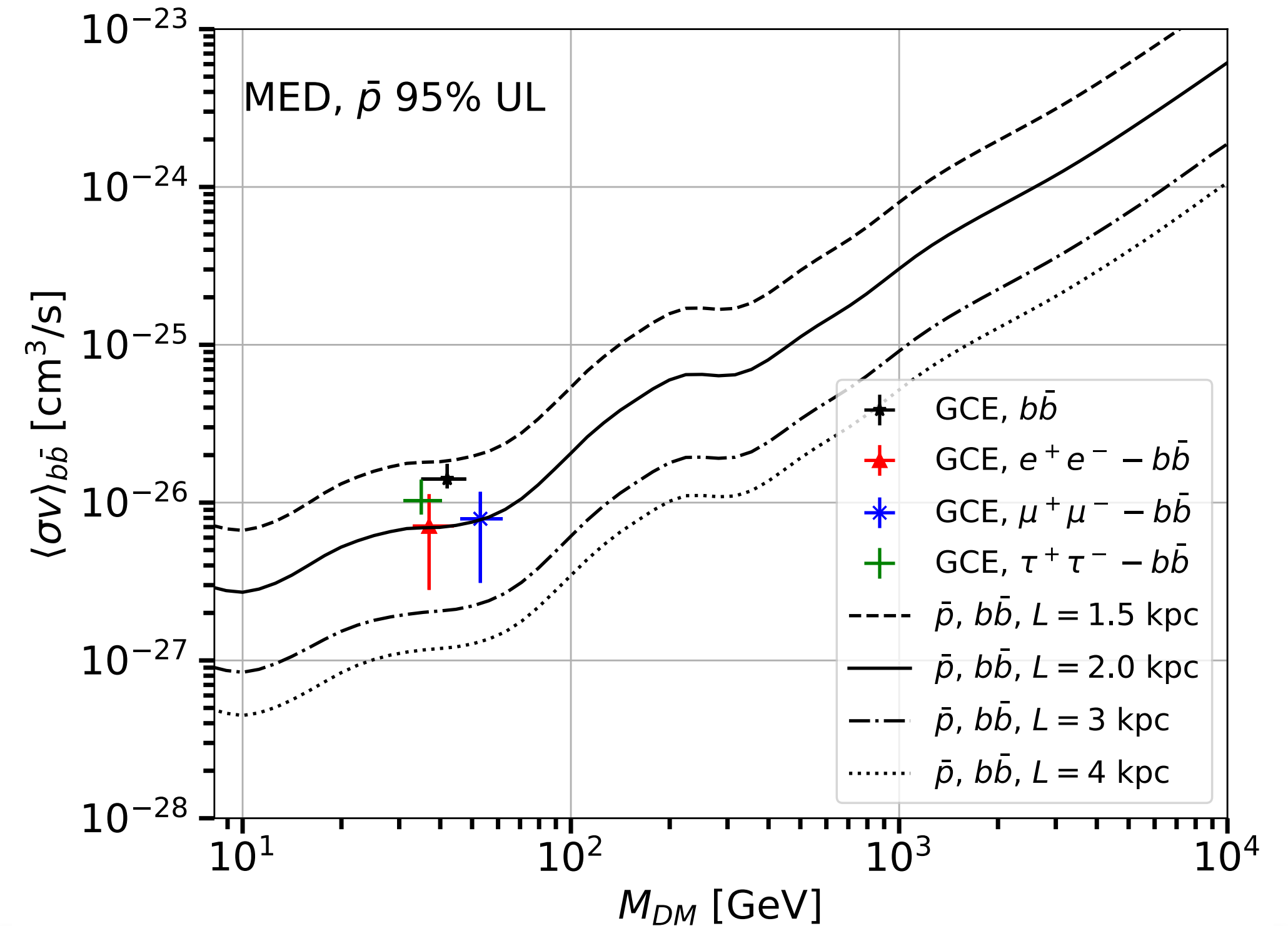
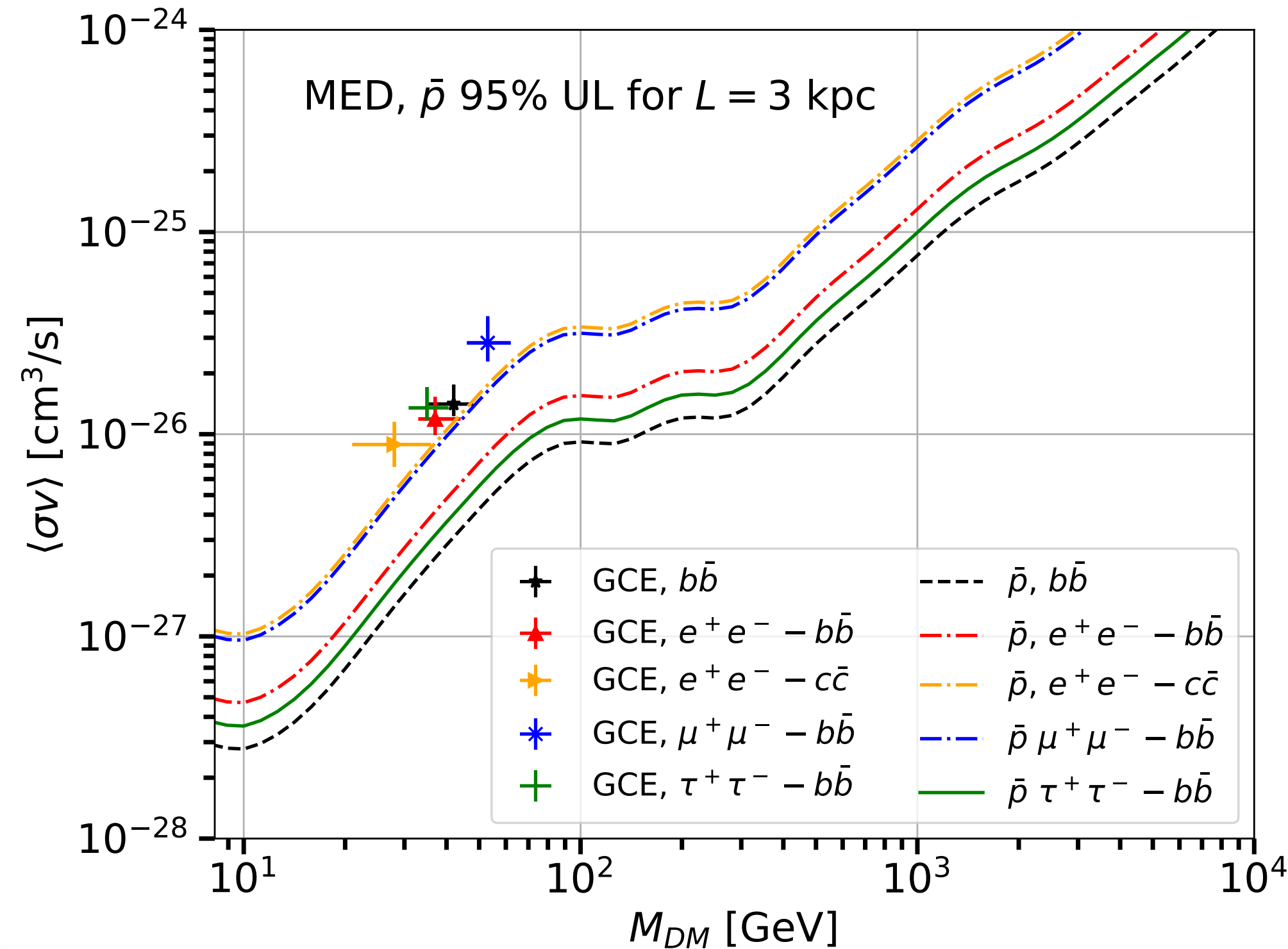
- We use the same analysis as in **Reinert and Winkler 2018**.
- A combined fit to AMS-02 and Voyager p, AMS-02 and Pamela anti-p, AMS-02 B/C is performed.

- $\delta = 0.459$
- $L = 4$ kpc (fixed)
- $K_0 = 0.042$ kpc²/Myr
- K_0/L should stay fixed
- Fisk potential I use $\phi = 0.72$ GV



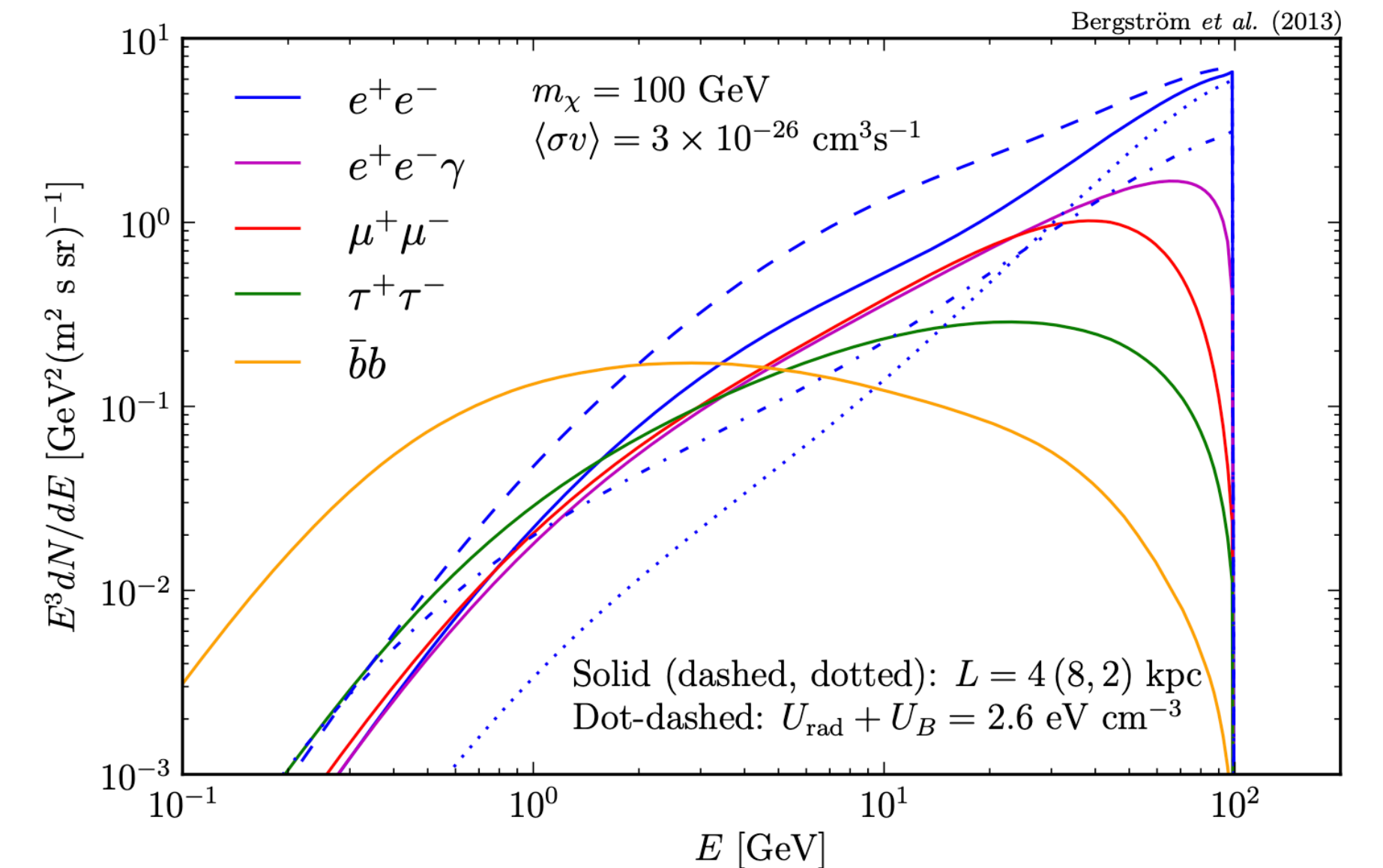
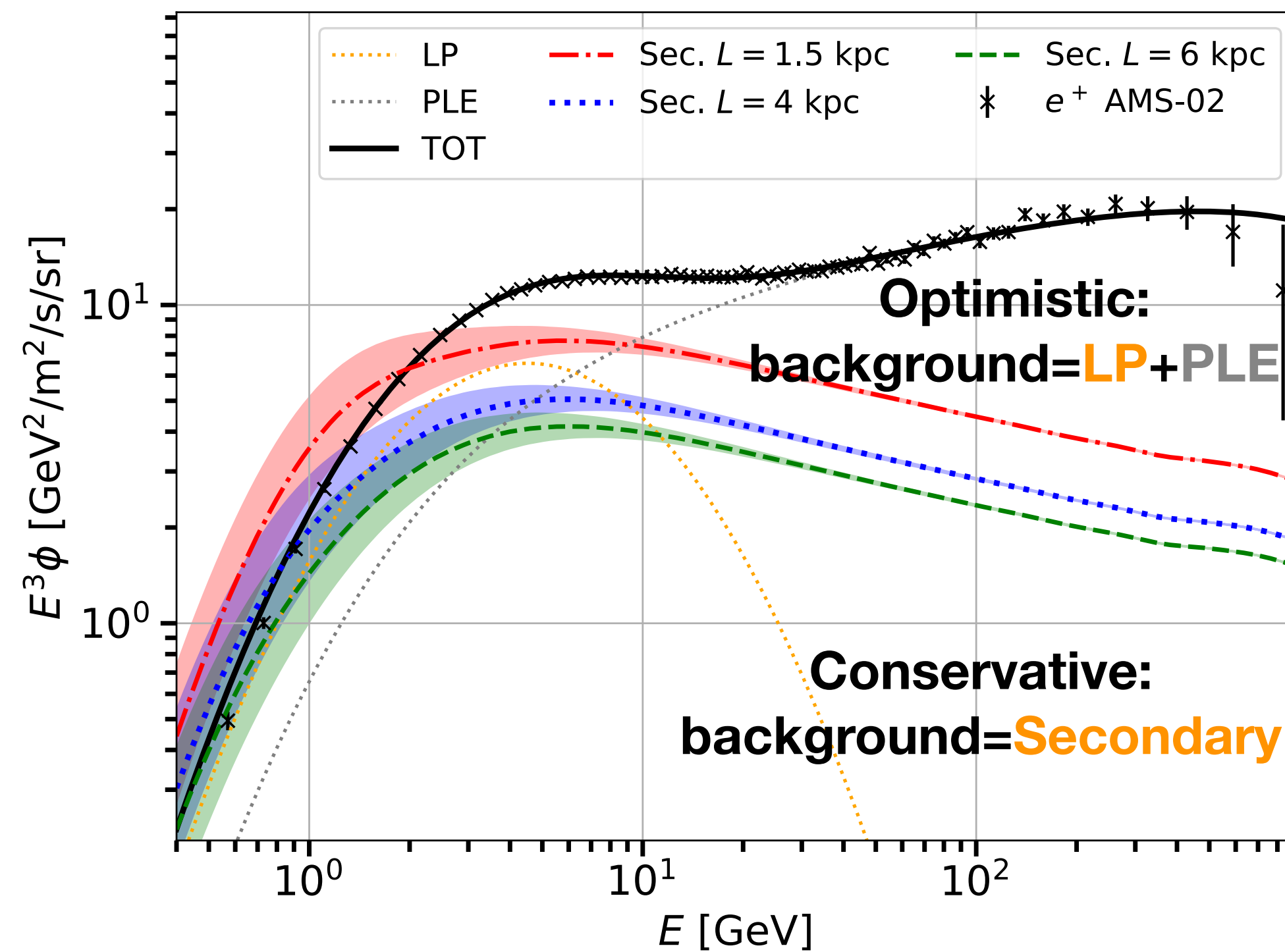
Antiprotons vs GCE

- GCE DM candidates with purely hadronic final states compatible with ULs only for $L < 1.8$ kpc.
- This constraints on L are relaxed for semi-hadronic final states with $L \leq 2.6$ kpc, respectively.
- ULs on L are $2-3\sigma$ below results obtained with latest radioactive CR data.



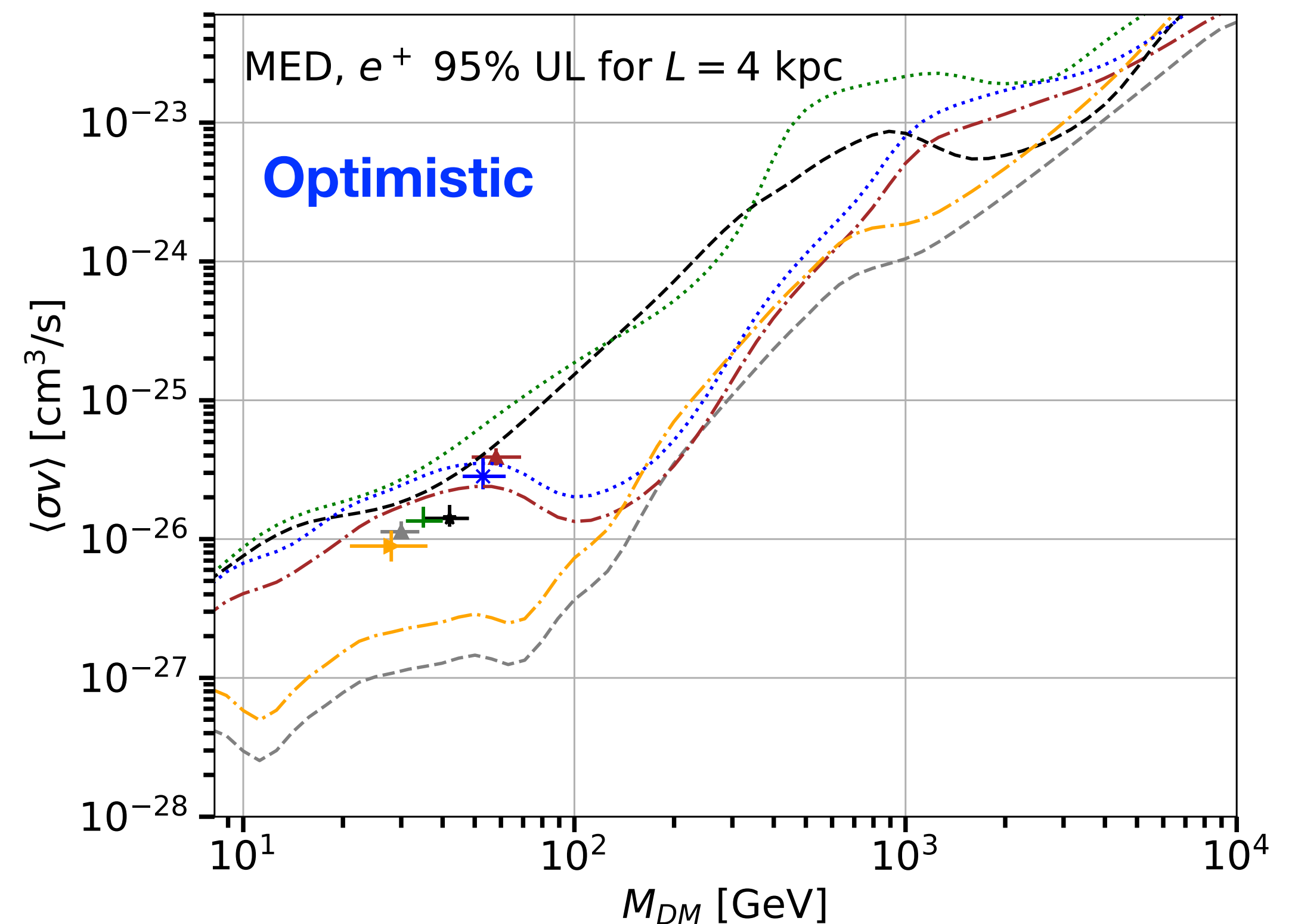
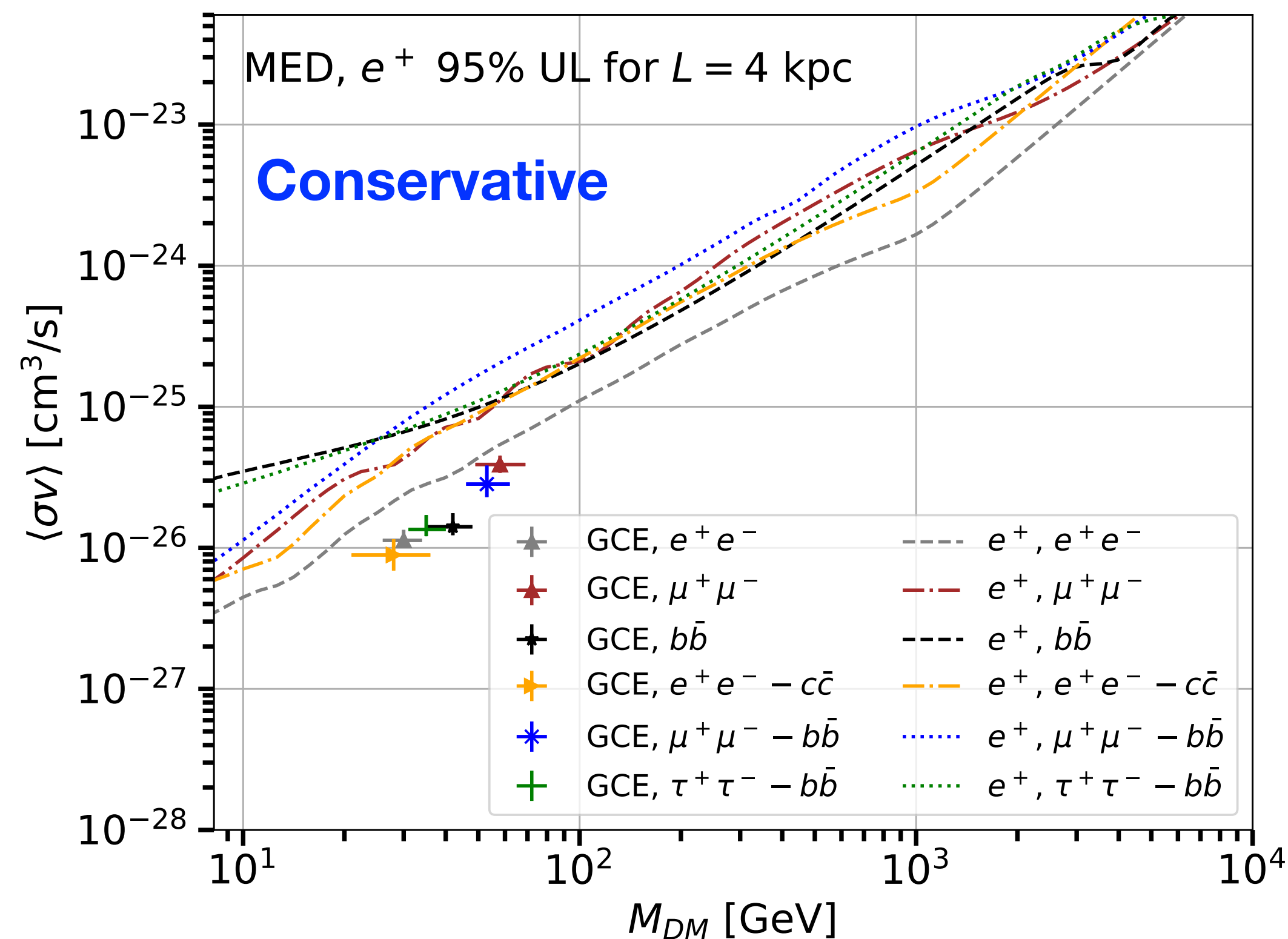
Cosmic-ray Positrons

- Low-energy positrons are primarily of secondary origin.
- Positrons above 10 GeV probably come from pulsar wind nebulae.
- We assumed a conservative and an optimist approach.



Positrons vs GCE

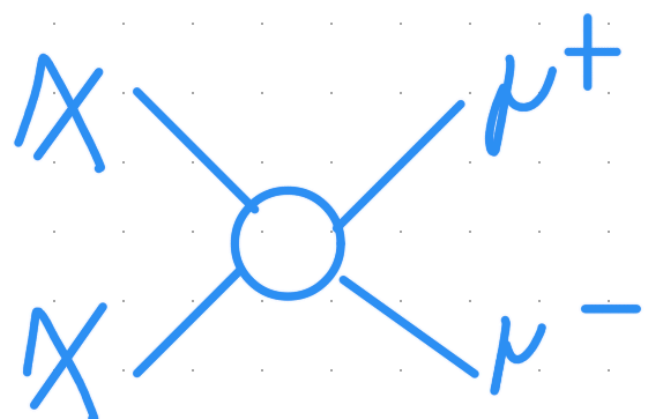
- The conservative upper limits are all compatible with the GCE.
- Instead, the optimistic ones are compatible for the bb , and mixed channels with muons and tau leptons.
- The channels with electrons are below the GCE DM candidates cross sections.



Summary of the DM interpretation

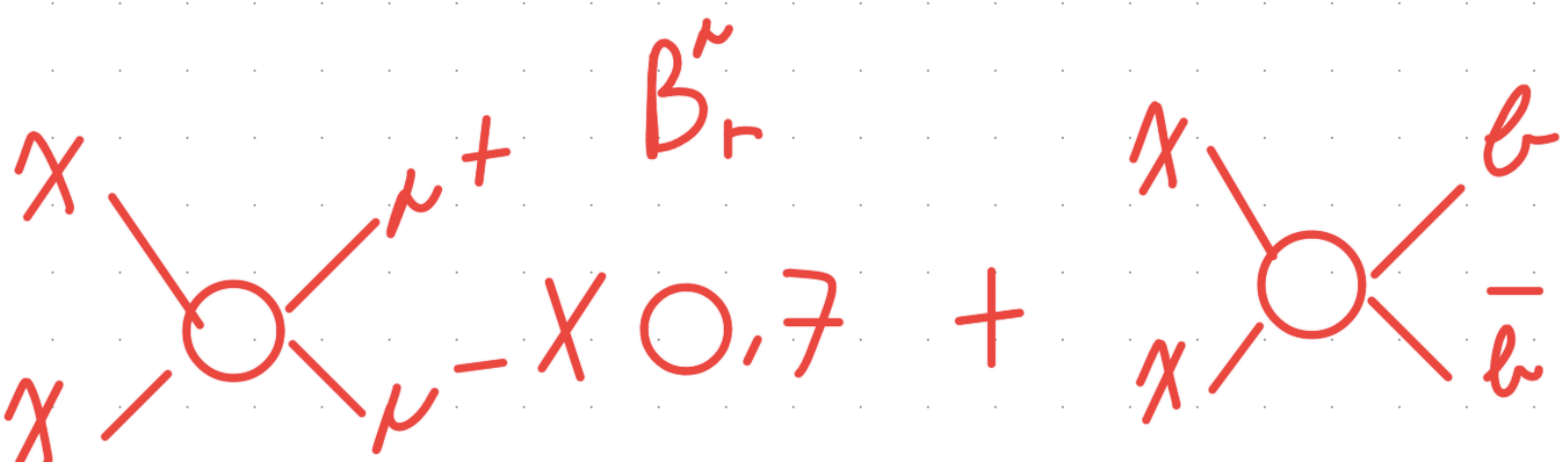
- The GCE has all the right characteristics to be due to annihilating DM particles.
- ULs from dSphs are compatible with the GCE candidates.
- ULs from antiprotons put tight constraints on purely hadronic final state DM.
- ULs from positrons put severe constraints on DM annihilating, even partially, into electrons.

1)



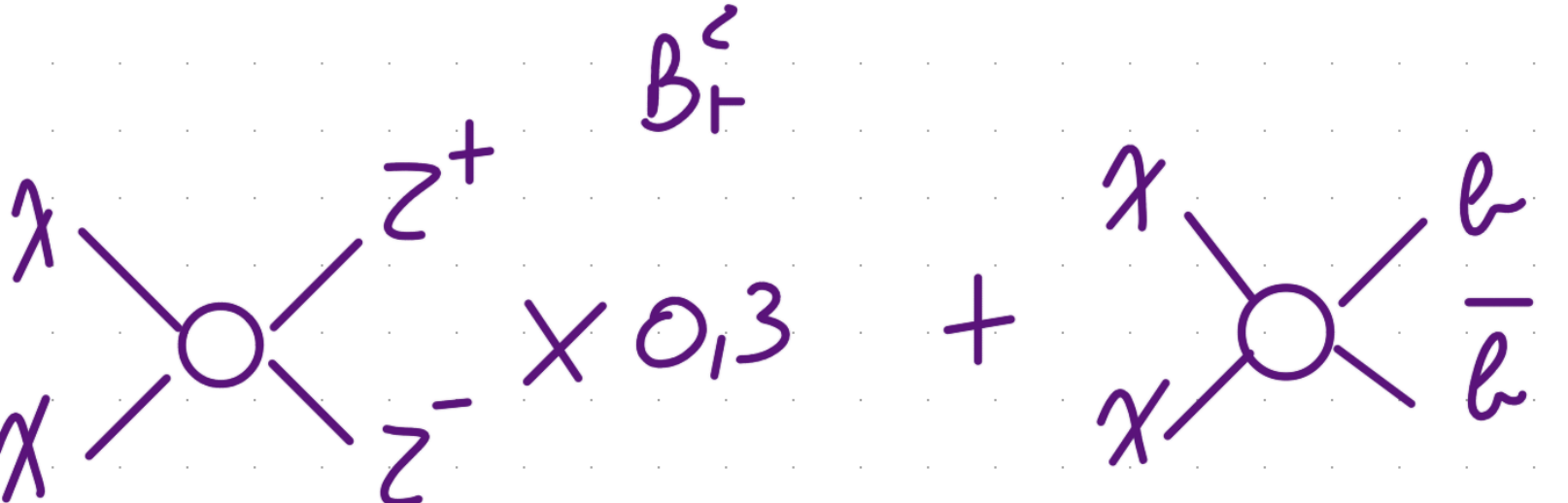
$M_X = 60 \text{ GeV}$
 $\langle \sigma v \rangle = 4 \cdot 10^{-26} \frac{\text{cm}^3}{\text{s}}$

2)



$B_r^{\mu} \quad M = 50 \text{ GeV}$
 $\langle \sigma v \rangle = 3 \cdot 10^{-26} \frac{\text{cm}^3}{\text{s}}$
 $L < 2,6 \text{ kpc}$

3)



$B_1^{\mu} \quad M = 35 \text{ GeV}$
 $\langle \sigma v \rangle = 1,4 \cdot 10^{-26} \frac{\text{cm}^3}{\text{s}}$
 $L < 1,8 \text{ kpc}$

Backup slides

Particle Physics Models with dark matter candidates

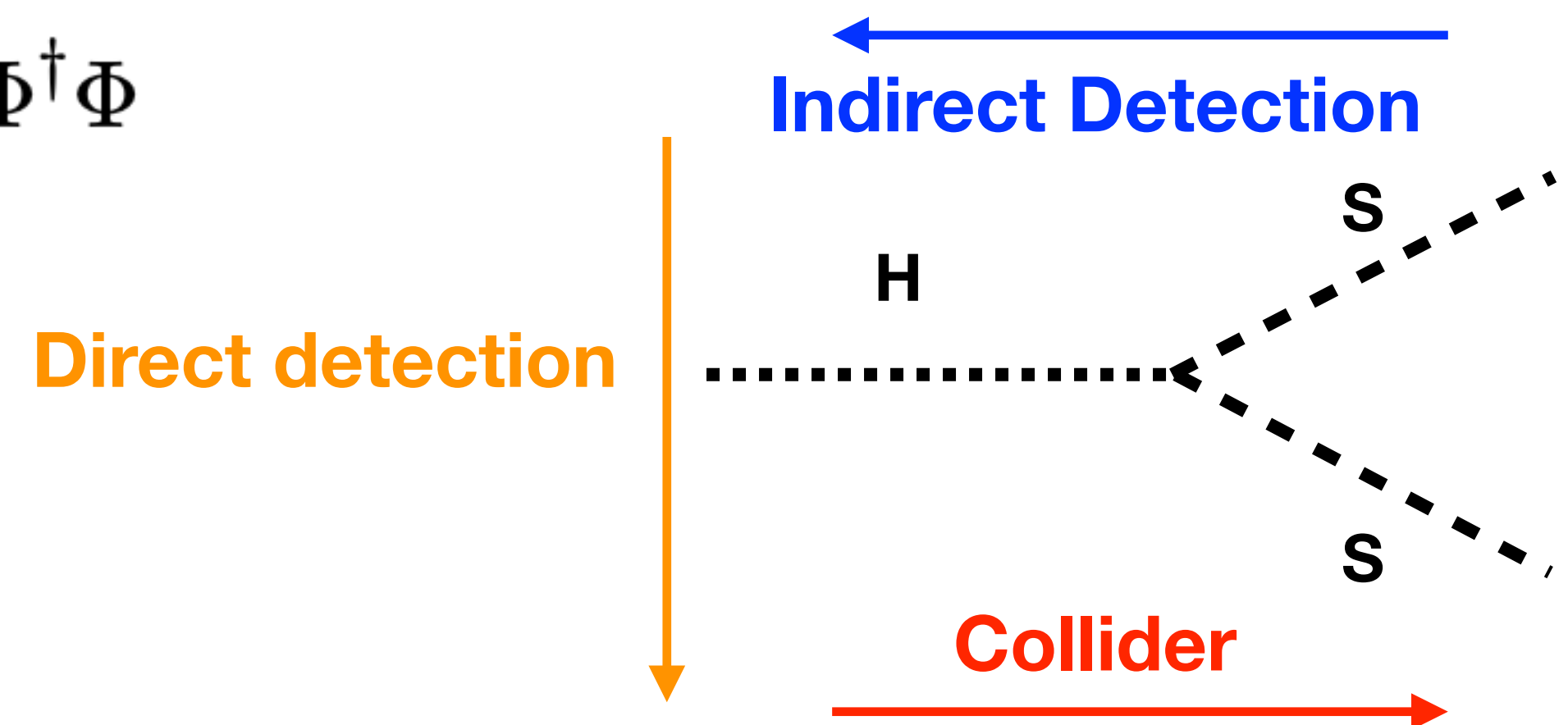
- Three possible categories of models:
 - Effective field theories
 - Simplified Models (DMsimps)
 - UV complete theories (SUSY)

DMsimps have the advantage to include the effect of the mediator between SM and BSM and to keep a limited number of parameters.

Scalar singlet Higgs portal model

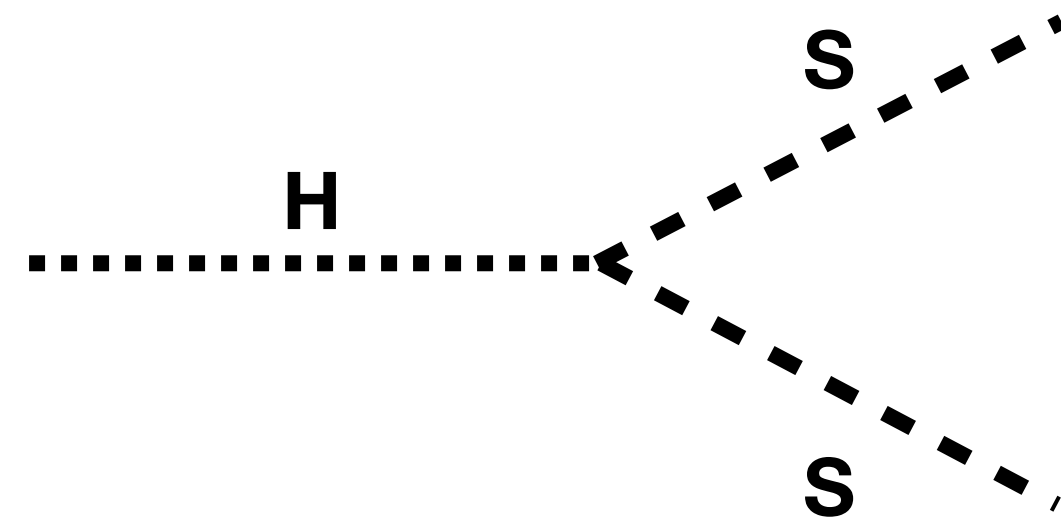
$$\mathcal{L} = \mathcal{L}_{\text{SM}} + \frac{1}{2} \partial_\mu S \partial^\mu S - \frac{1}{2} m_{S,0}^2 S^2 - \frac{1}{4} \lambda_S^2 S^4 - \frac{1}{2} \lambda_{\text{HP}} S^2 \Phi^\dagger \Phi$$

$$\mathcal{L}_{\text{HP}} = -\frac{1}{4} \lambda_{\text{HP}} h^2 S^2 - \frac{1}{2} \lambda_{\text{HP}} v h S^2$$



Collider and indirect detection

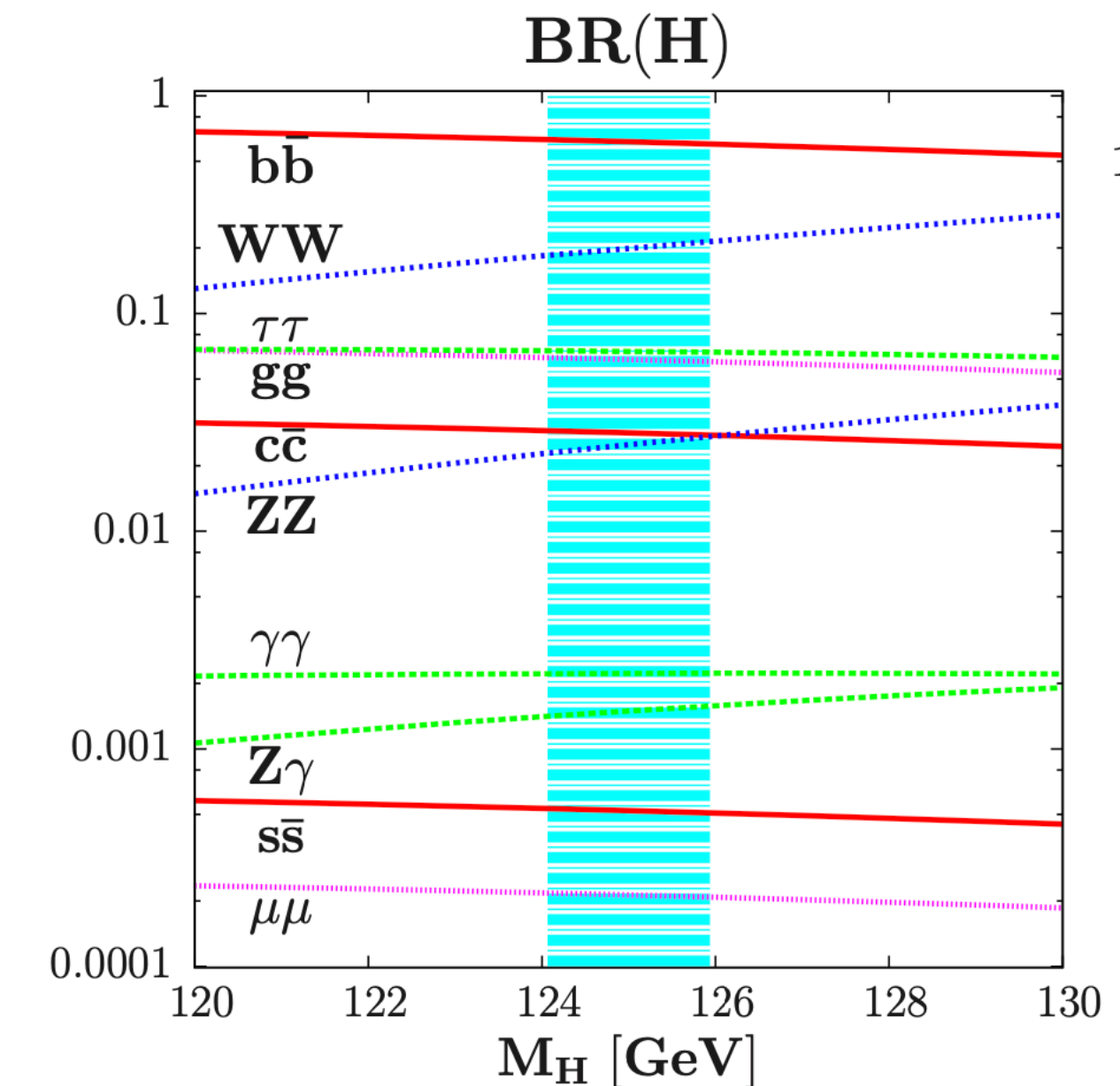
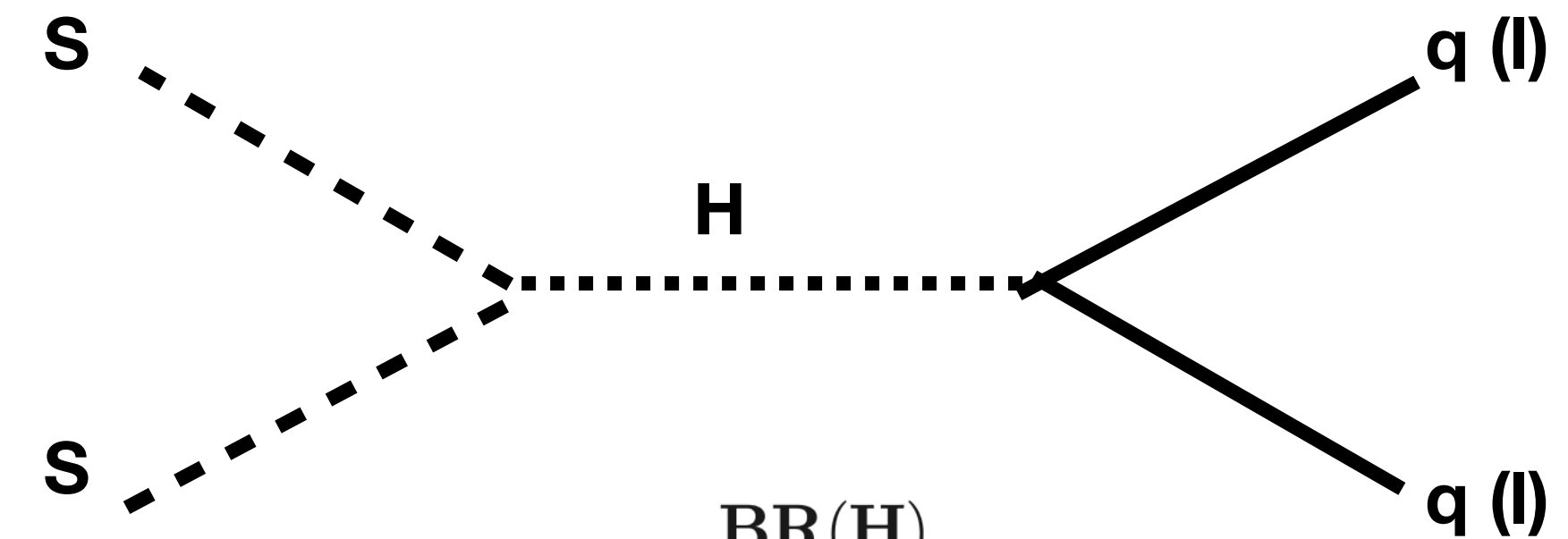
Collider searches: Invisible Higgs decay.



$$\Gamma_{\text{inv}} = \frac{\lambda_{\text{HP}}^2 v^2}{32\pi m_h} \sqrt{1 - 4 \frac{m_S^2}{m_h^2}}$$

- Recent ATLAS/CMS measurements (2022):
 - ATLAS <0.145 and CMS <0.180
 - Combined <0.10** ([WebLink](#), no paper?)

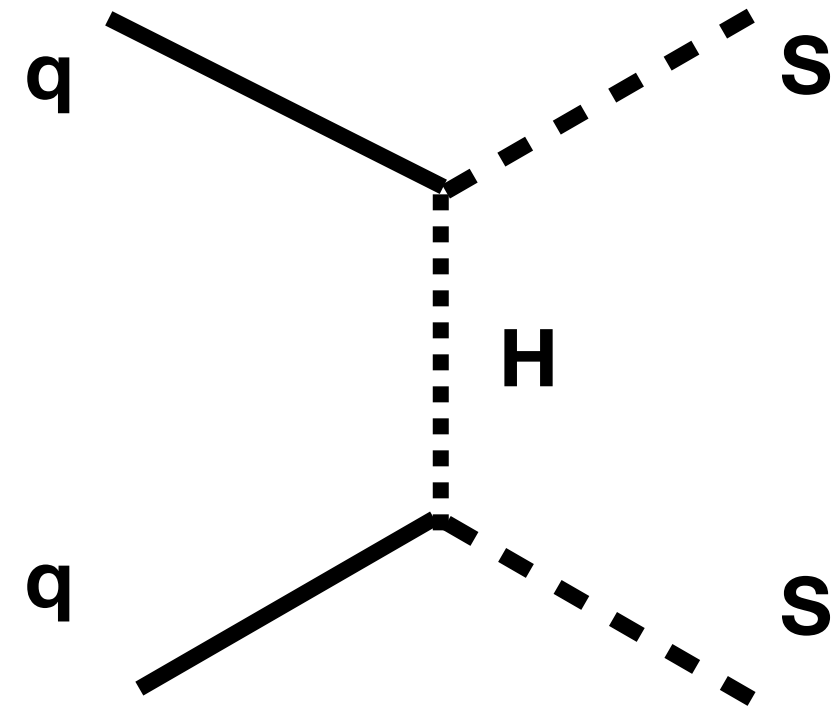
Indirect detection



- Production of gamma rays and antiprotons through hadronization (Fermi-LAT and AMS-02 data).

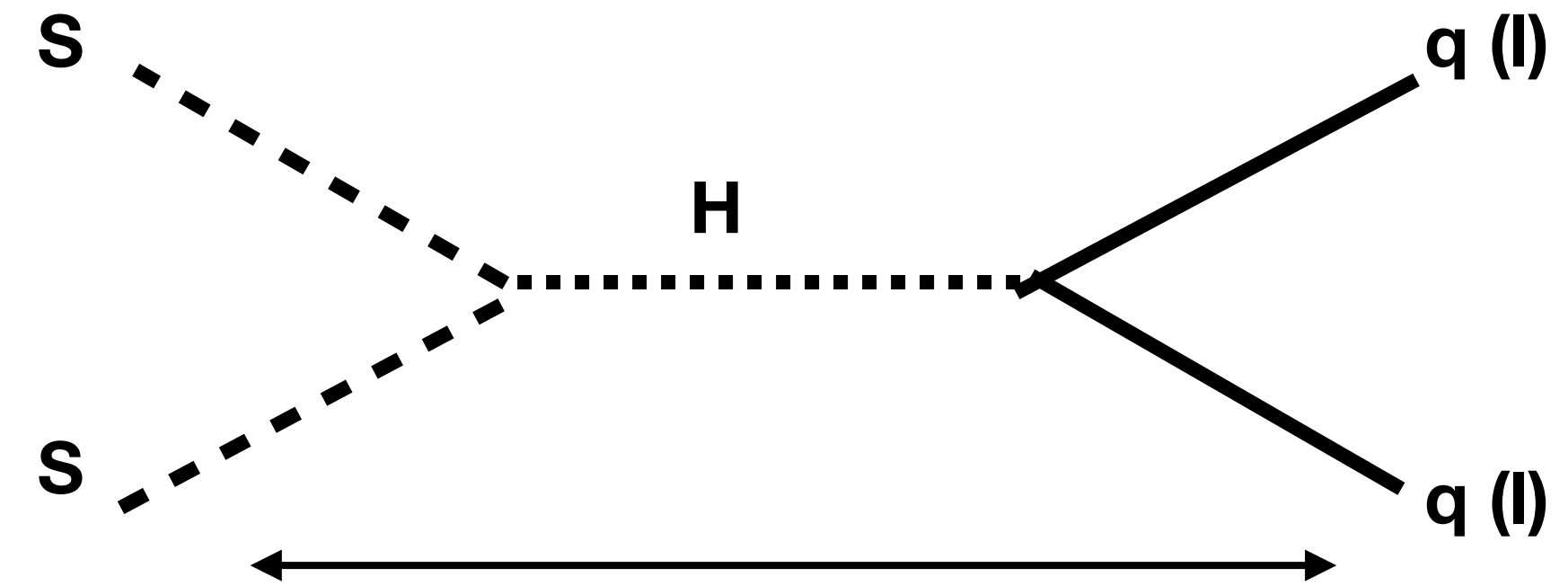
Direct detection and relic density

Direct detection

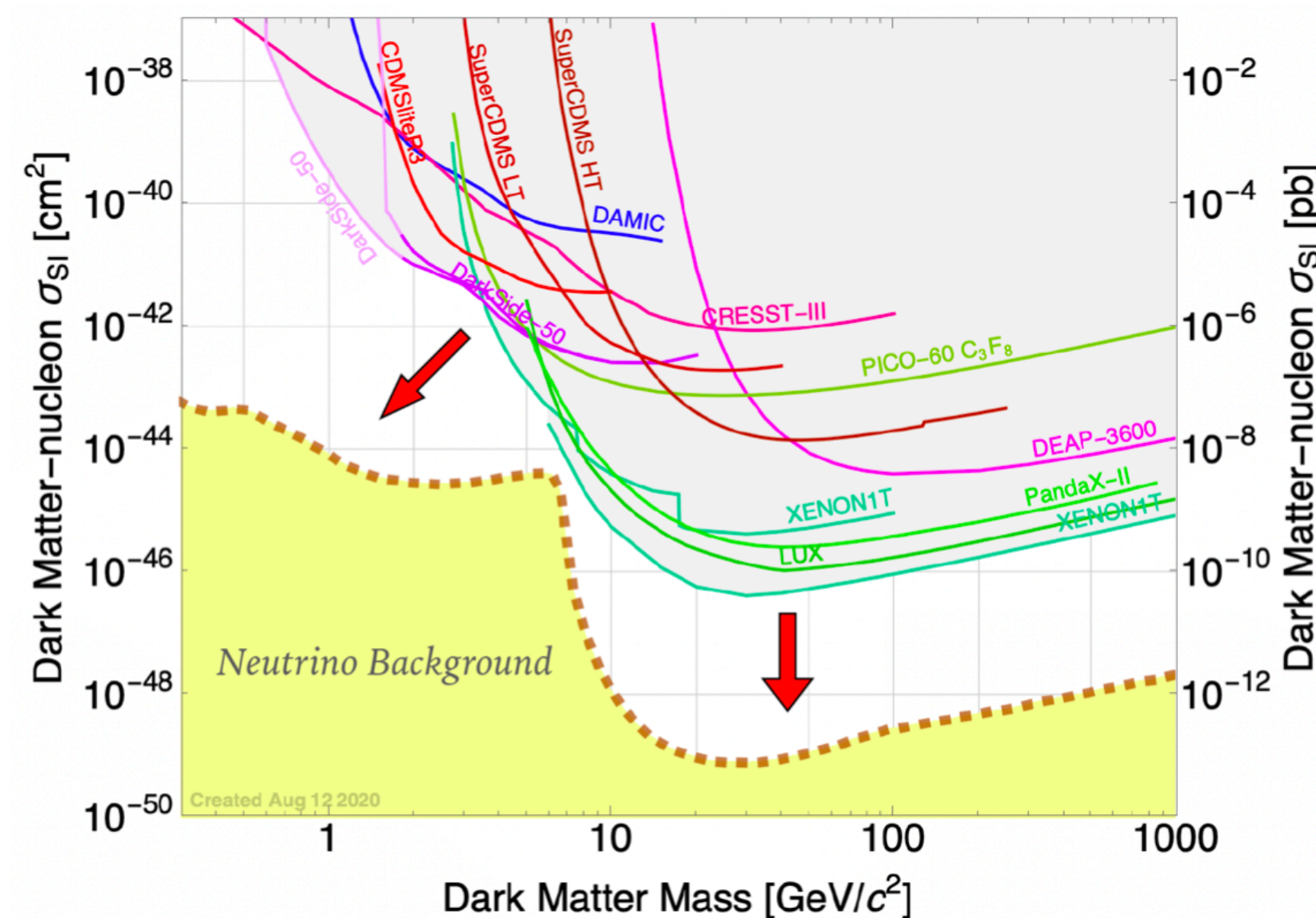


$$\sigma_{sN}^{\text{SI}} = \frac{\lambda_{Hss}^2}{16\pi M_H^4} \frac{m_N^4 f_N^2}{(M_s + m_N)^2}$$

Relic density

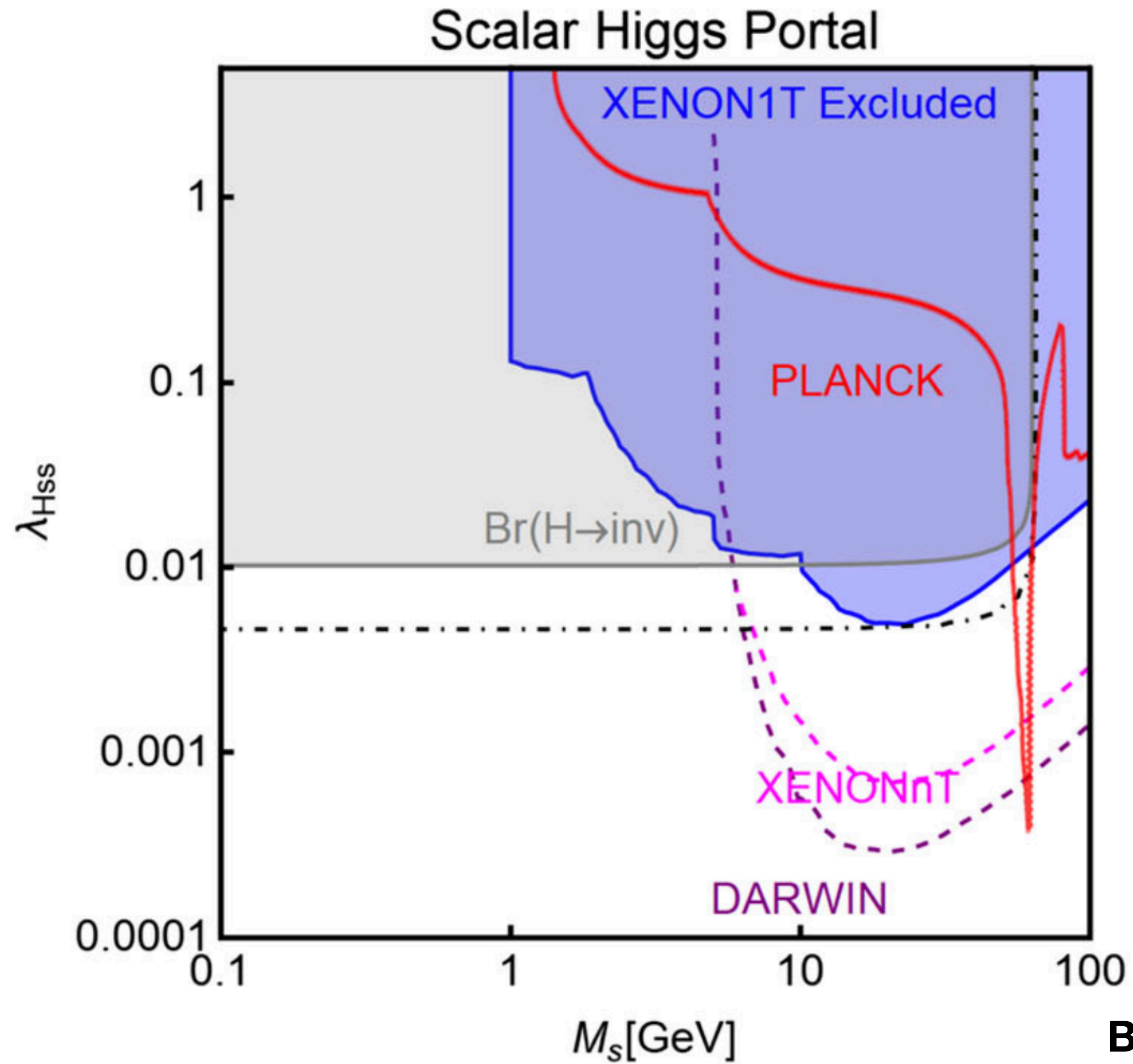


$$\Omega_{\text{DM}} h^2 = 0.1188 \pm 0.0010$$



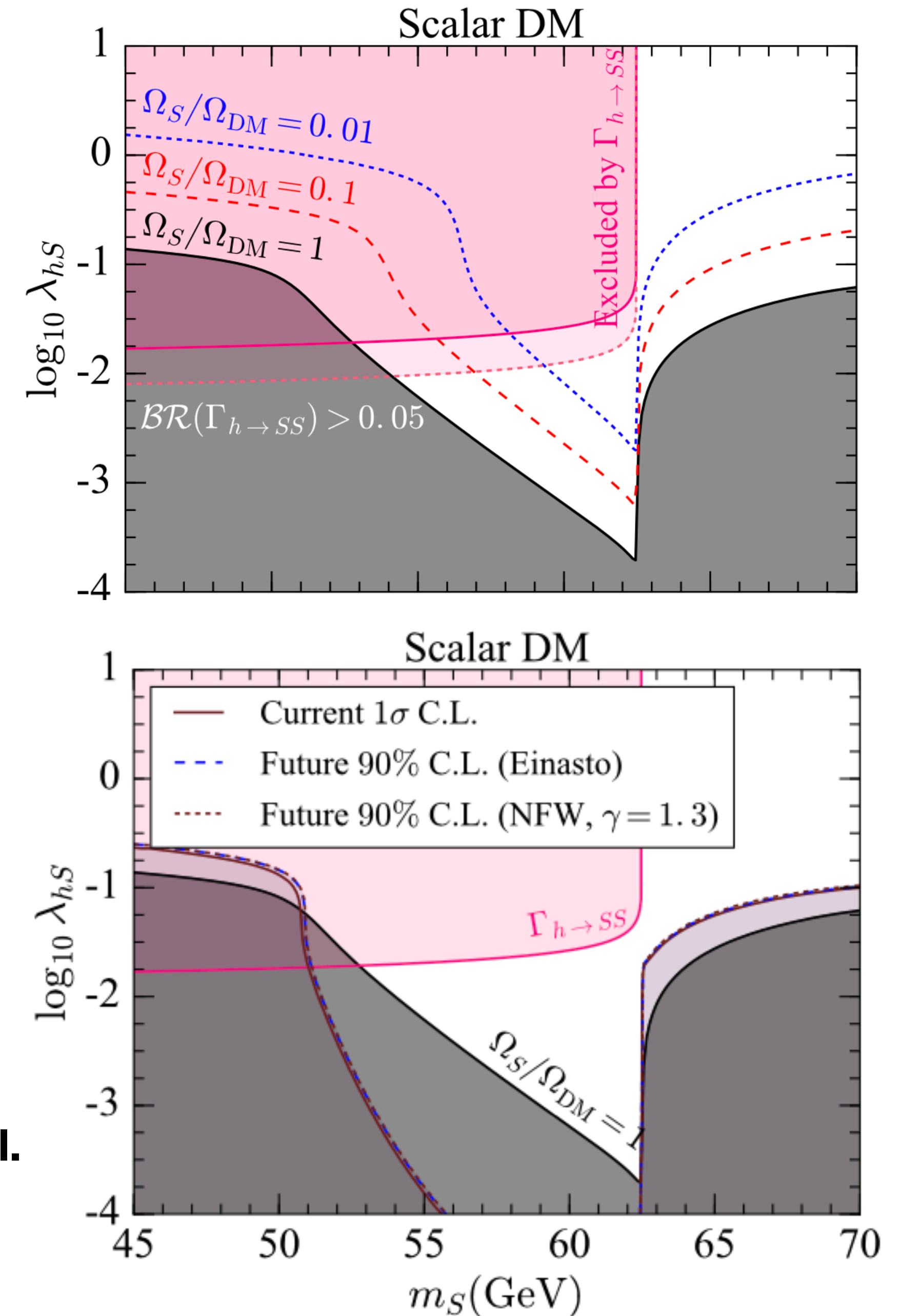
- This one of the highest constraints available.
- Different model could bring to this relic density:
 - Freeze-out
 - Freeze-in

Putting all together.....



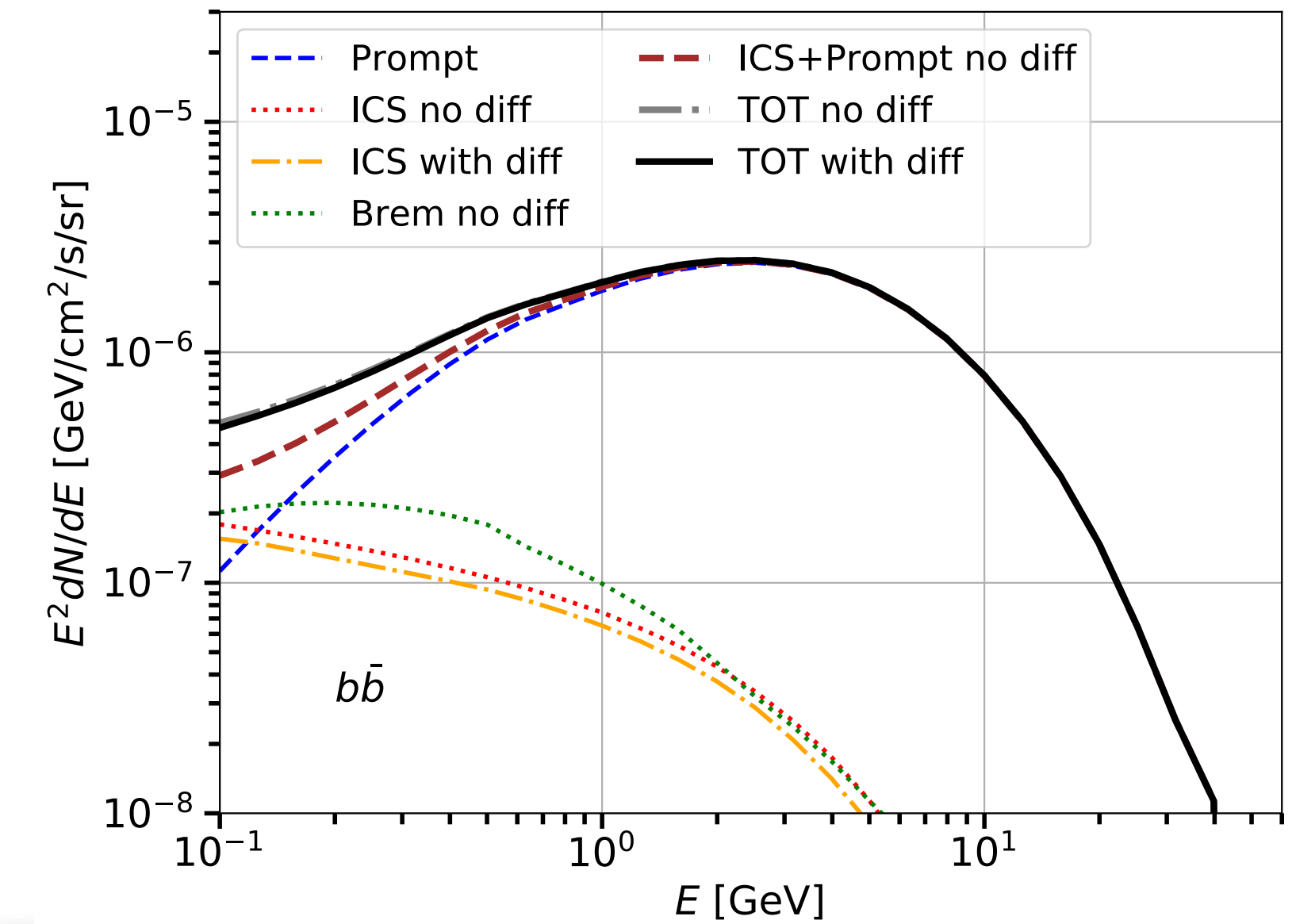
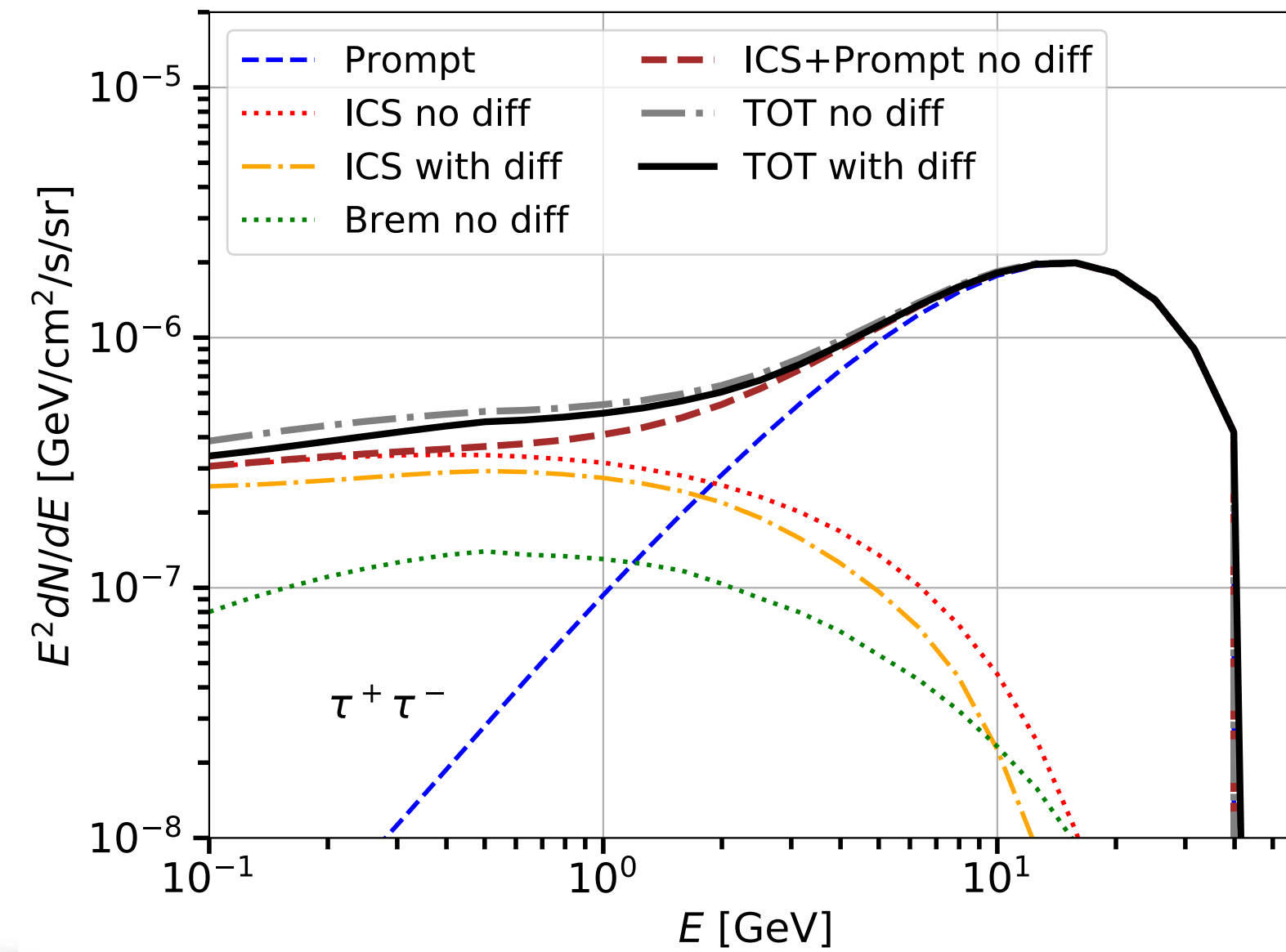
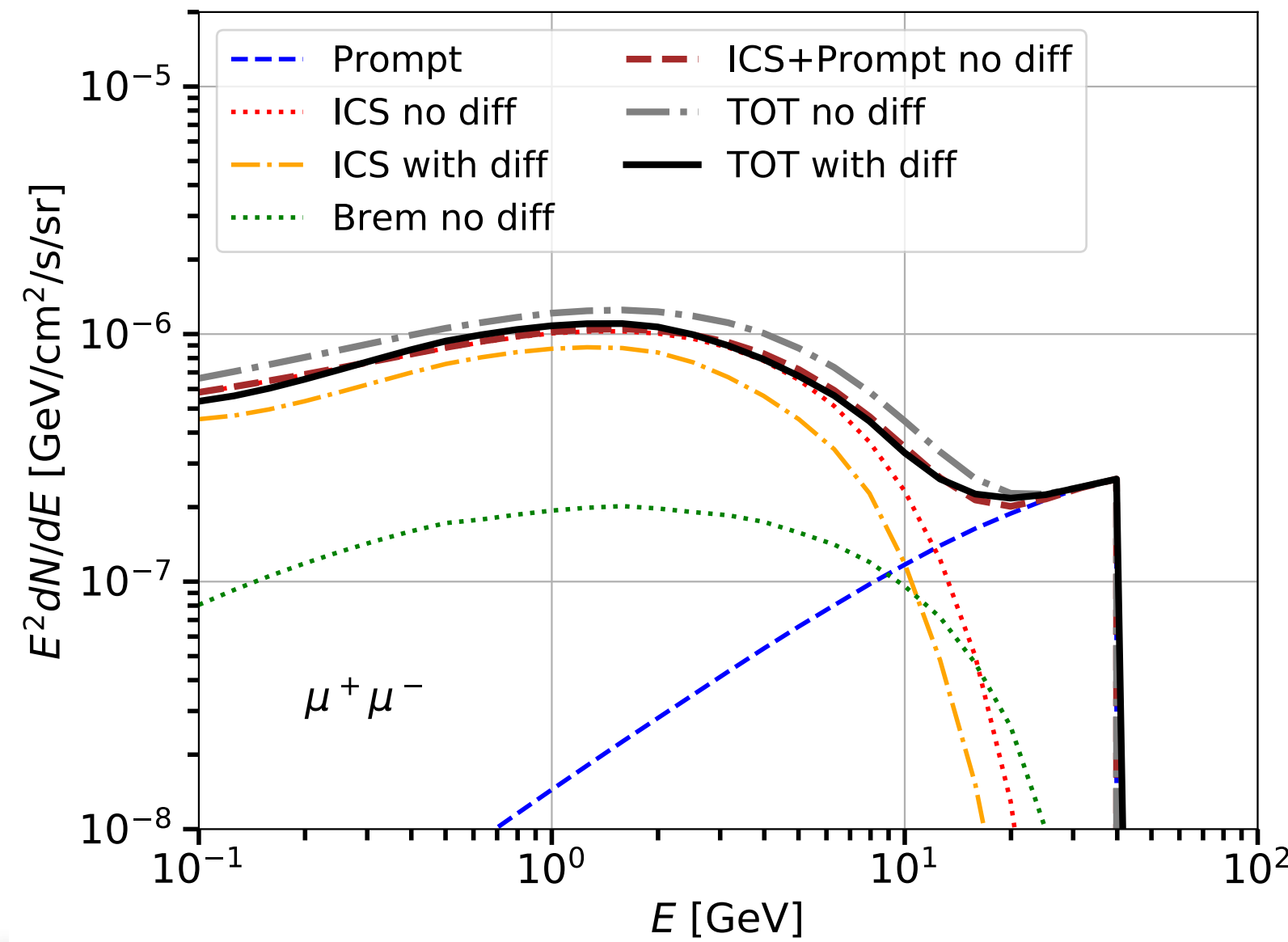
Arcadi et al. 2021

Beniwal et al.
2016



Theory for the gamma-ray flux from Dark matter

- We use a model that accounts for prompt and ICS emission from DM.
- The diffusion process has a much smaller effect than energy losses in the GC.
- The bremsstrahlung component is also negligible.



Cosmic-ray antiprotons

Diffusion

$$K = K_0 \beta^\eta \left(\frac{\mathcal{R}}{\text{GV}} \right)^\delta \left(1 + \left(\frac{\mathcal{R}}{\mathcal{R}_b} \right)^{\Delta\delta/s} \right)^{-s}$$

Energy losses

$$b_{\text{disc}} = b_{\text{coul}} + b_{\text{ion}} + b_{\text{brems}} + b_{\text{reac}}$$

Reacceleration

$$K_{EE} = \frac{4}{3} \frac{V_a^2}{K} \frac{p^2}{\delta(4-\delta)(4-\delta^2)}$$

Annihilation rate

$$-K \Delta \mathcal{N}_i + 2h\delta(z) \left[\partial_E (b_{\text{disc}} \mathcal{N}_i - K_{EE} \partial_E \mathcal{N}_i) + \Gamma_{\text{ann}} \mathcal{N}_i \right] + \partial_E (b_{\text{halo}} \mathcal{N}_i) = 2h\delta(z) \mathcal{Q}_i^{\text{sec}} + \mathcal{Q}_i^{\text{prim}} .$$

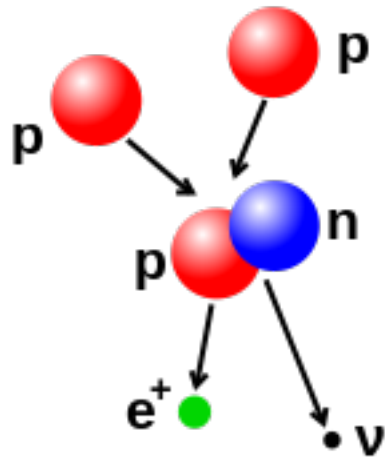
$$b_{\text{halo}} = b_{\text{ic}} + b_{\text{synch}}$$

Energy losses

$$\mathcal{Q}_i^{\text{sec}} = \sum_{j,k} 4\pi \int dE' \left(\frac{d\sigma_{jk \rightarrow i}}{dE} \right) n_k \Phi_j(E')$$

Secondary

Primary

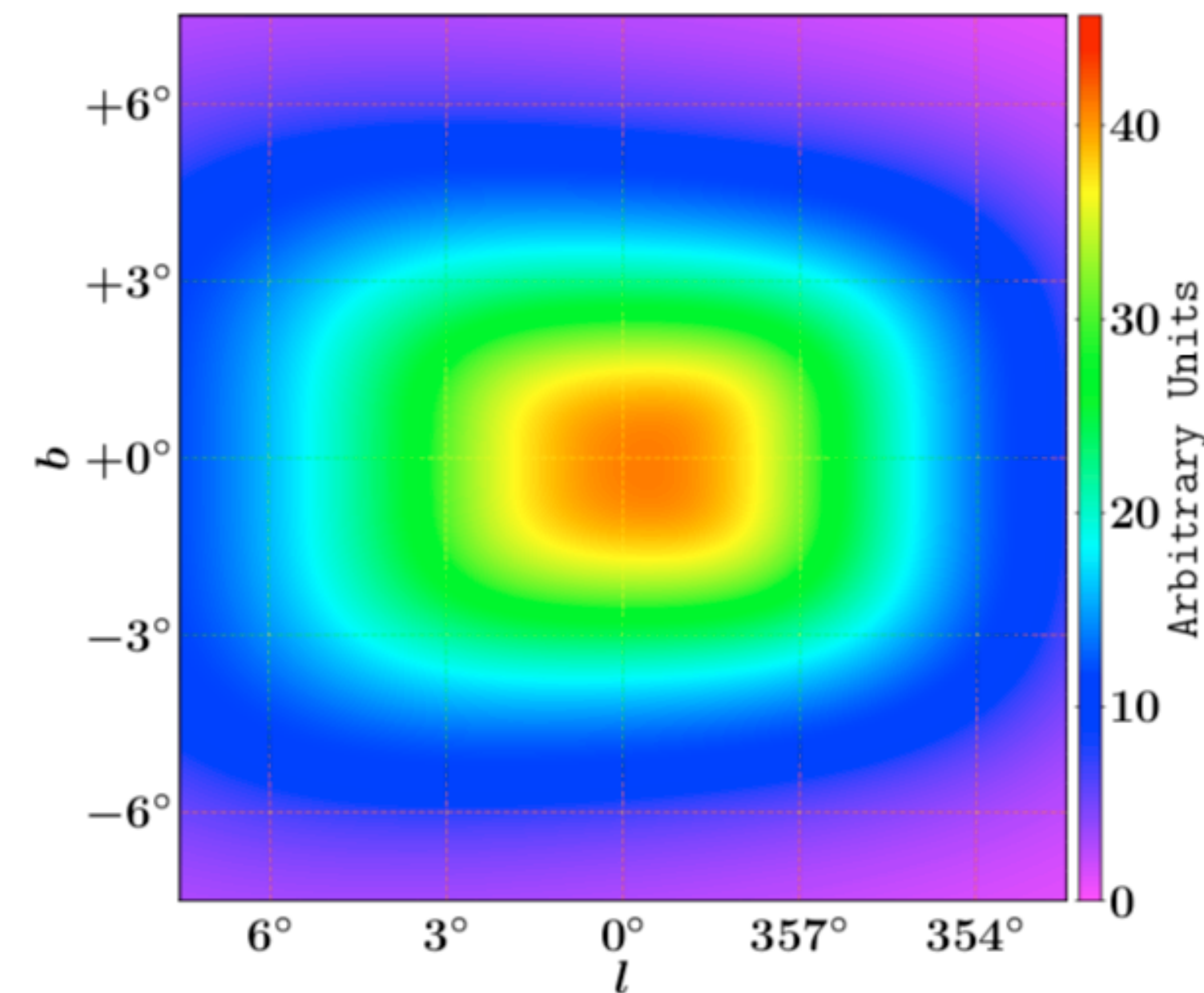
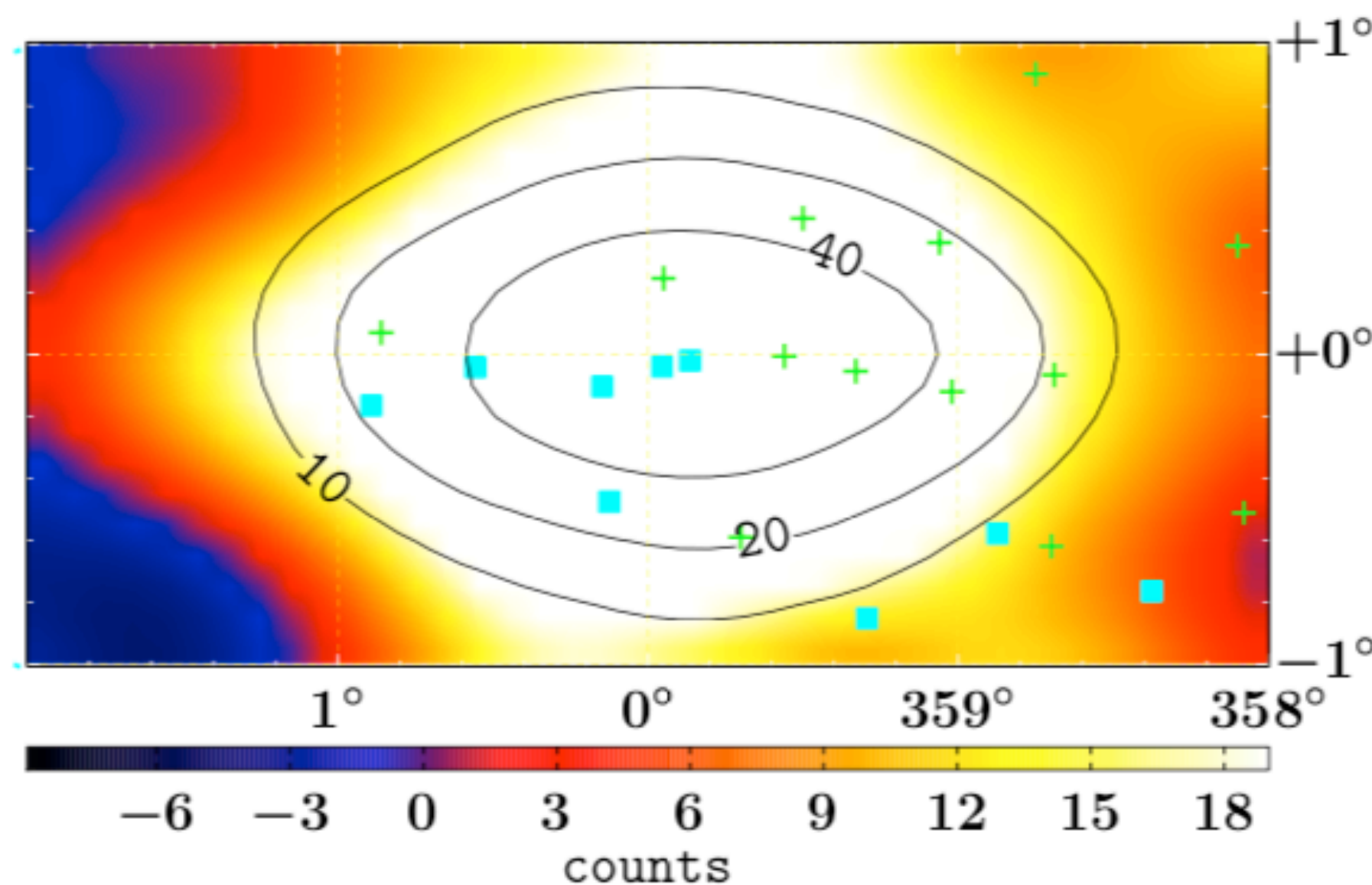


L vertical size of the diffusive halo

Galactic bulge

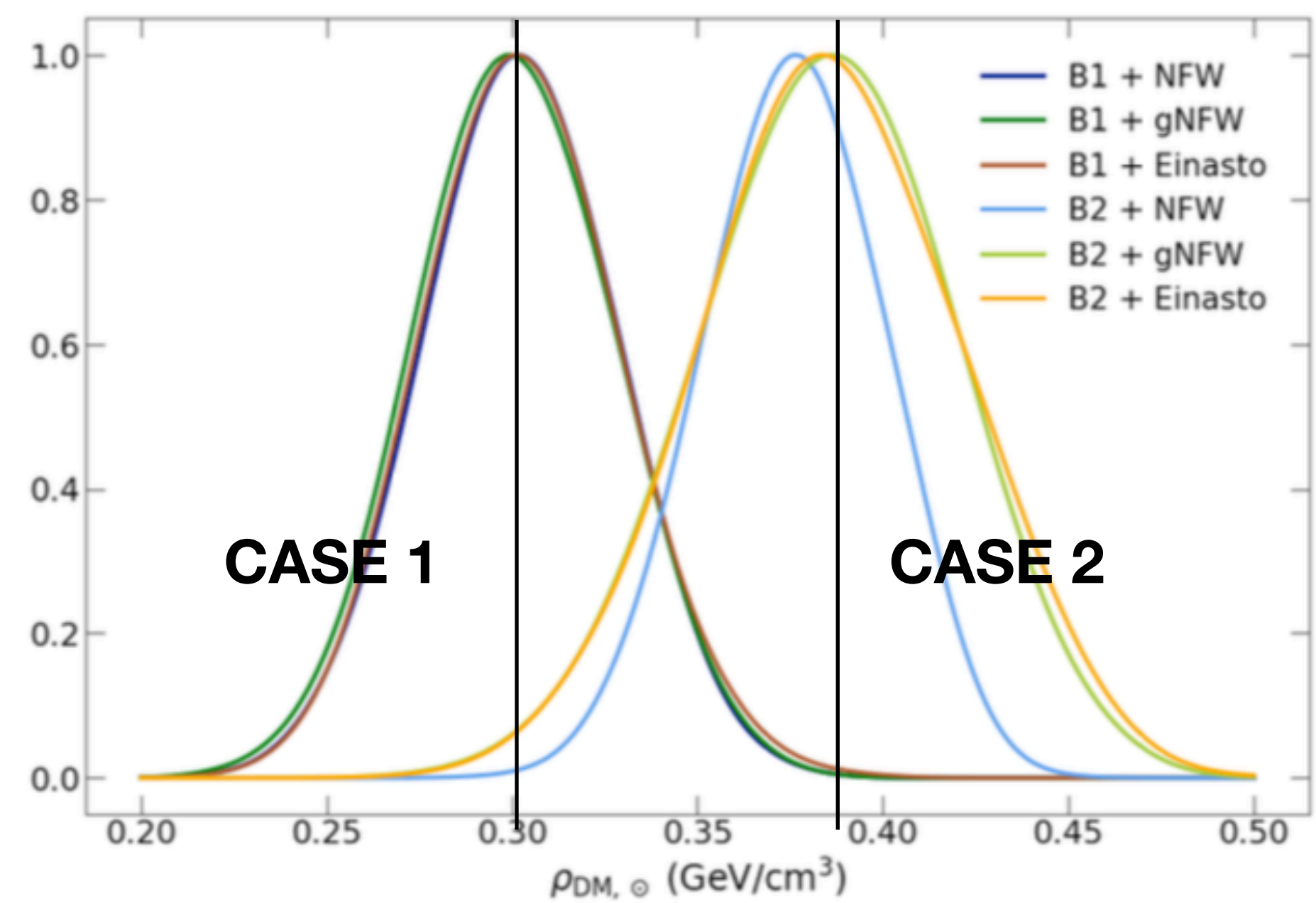
- **Macias et al. 2016-2020:**

- The GCE is better described by the stellar over-density in the Galactic bulge and the nuclear stellar bulge, rather than a spherical excess.
- Given its non-spherical nature, they argue that the GCE is not a dark matter phenomenon but rather associated with the stellar population of the Galactic bulge and nuclear bulge.



Choosing the local DM density

Salas et al. 2019



	NFW	gNFW	Einasto
M_{200} [$10^{11} M_{\odot}$]	$5.2^{+2.0}_{-1.1}$	$5.5^{+3.1}_{-1.4}$	$2.8^{+7.7}_{-1.2}$
c_{200}	15^{+5}_{-4}	14 ± 5	12 ± 4
Slope parameter	$\gamma = 1$	$\gamma = 1.2^{+0.3}_{-0.8}$	$\alpha = 0.11^{+0.20}_{-0.05}$
$\rho_{\text{DM}, \odot}$ [GeV/cm^3]	$0.301^{+0.028}_{-0.025}$	$0.300^{+0.028}_{-0.027}$	0.301 ± 0.027
r_{200} [kpc]	173^{+19}_{-13}	174^{+29}_{-15}	182^{+43}_{-51}
r_s [kpc]	10^{+5}_{-3}	9^{+12}_{-8}	11^{+10}_{-4}

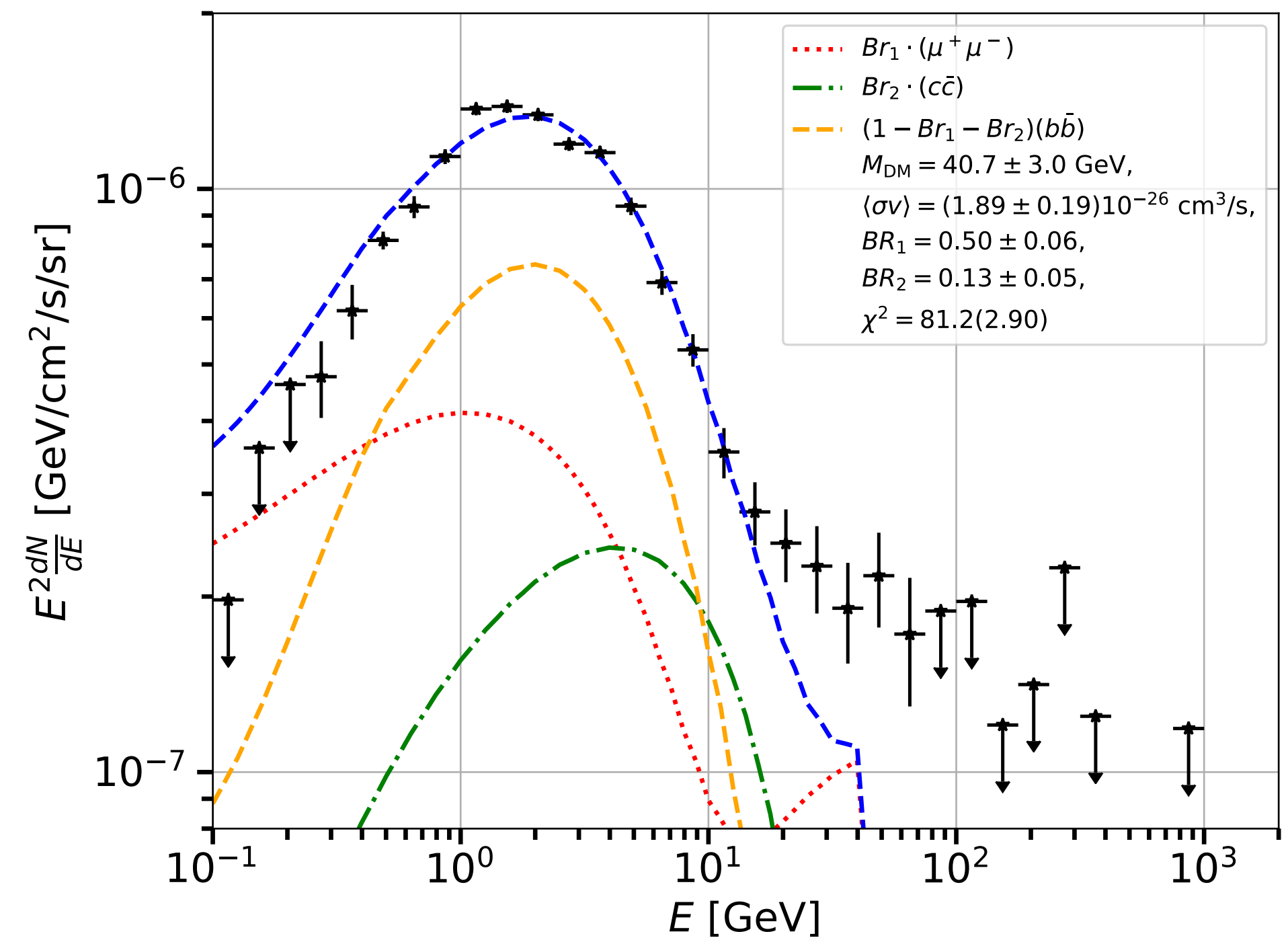
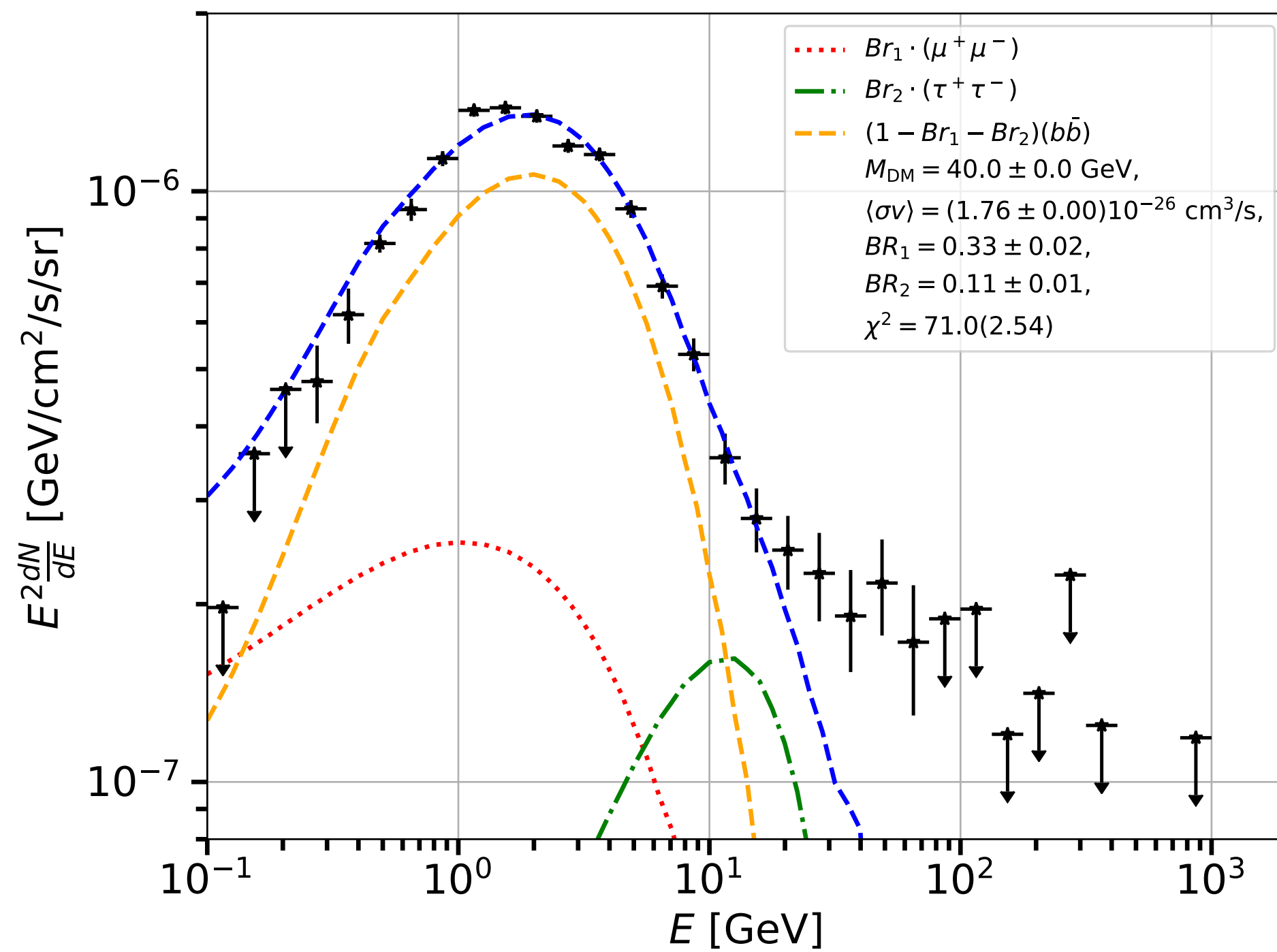
CASE 1

	NFW	gNFW	Einasto
M_{200} [$10^{11} M_{\odot}$]	$7.4^{+1.8}_{-1.5}$	$6.3^{+3.4}_{-1.3}$	$3.0^{+5.7}_{-1.2}$
c_{200}	16^{+4}_{-3}	17 ± 6	14^{+5}_{-4}
Slope parameter	$\gamma = 1$	$\gamma = 1.3^{+0.3}_{-0.9}$	$\alpha = 0.18^{+0.21}_{-0.09}$
$\rho_{\text{DM}, \odot}$ [GeV/cm^3]	0.376 ± 0.025	$0.387^{+0.034}_{-0.036}$	$0.384^{+0.038}_{-0.034}$
r_{200} [kpc]	192^{+15}_{-13}	184^{+29}_{-14}	147^{+59}_{-19}
r_s [kpc]	11^{+4}_{-3}	$8.1^{+10.6}_{-7.8}$	$9.2^{+5.3}_{-2.7}$

CASE 2

Fitting the GCE data with three channels

Channel 1	Channel 2	Channel 3	M_{DM} [GeV]	$\langle\sigma v\rangle$ [10^{-26} cm ² /s]	BR_1	BR_2	$\chi^2(\tilde{\chi}^2)$	$\Delta\chi^2(sign.)$
e^+e^-	$\mu^+\mu^-$	$b\bar{b}$	43.87 ± 2.72	2.05 ± 0.23	0.08 ± 0.06	0.54 ± 0.07	87.8(3.14)	2.7
e^+e^-	$\tau^+\tau^-$	$b\bar{b}$	35.17 ± 1.56	1.28 ± 0.07	0.07 ± 0.10	0.18 ± 0.03	81.6	0.40
$\mu^+\mu^-$	$\tau^+\tau^-$	$b\bar{b}$	40.00 ± 1.75	1.76 ± 0.12	0.32 ± 0.08	0.11 ± 0.06	71.0	11.0(3.1 σ)
$\mu^+\mu^-$	$c\bar{c}$	$b\bar{b}$	40.66 ± 3.28	1.89 ± 0.19	0.50 ± 0.06	0.13 ± 0.05	81.2(2.90)	9.3(2.8 σ)



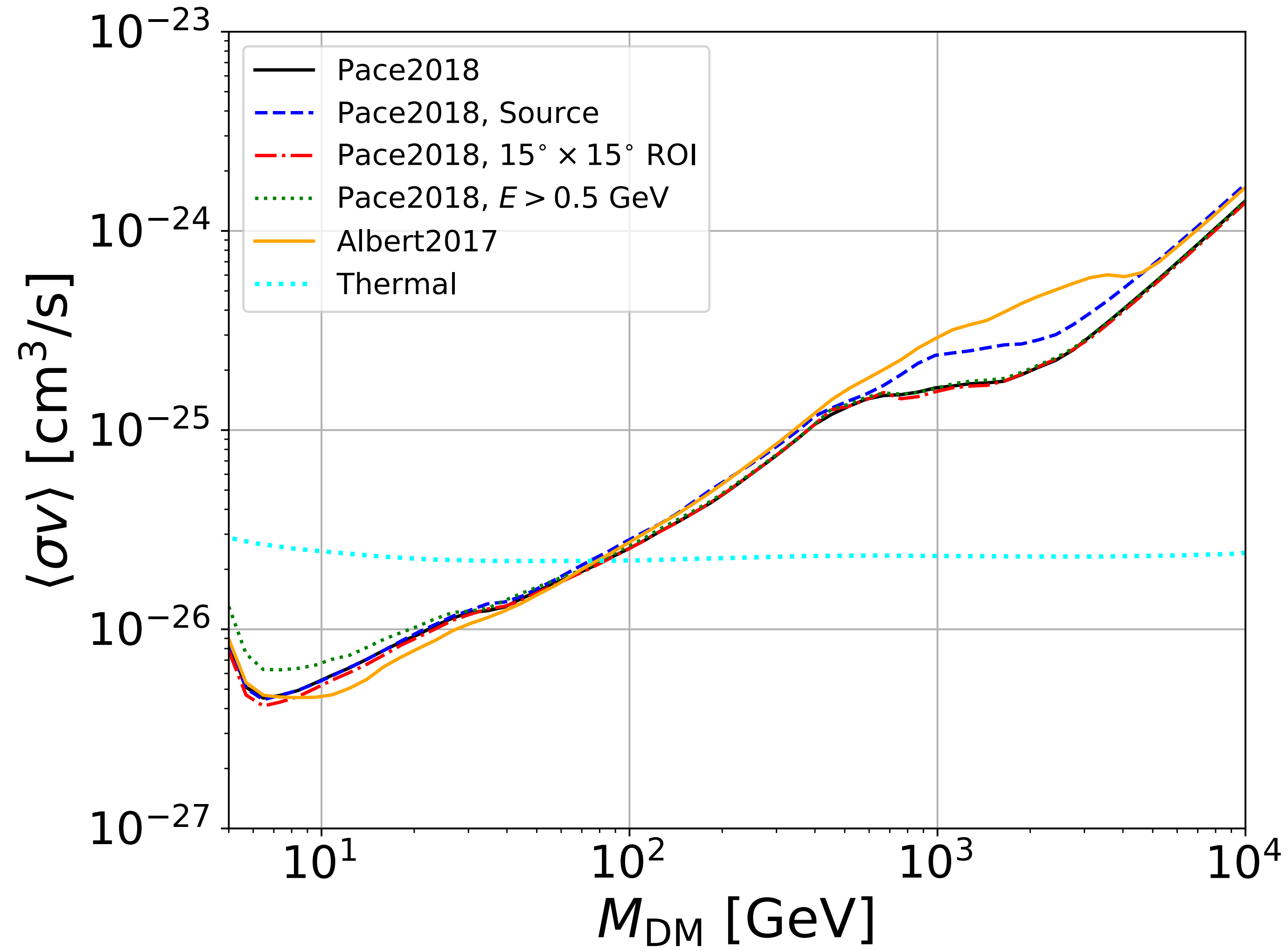
Analysis of the dSphs

- Alex D.W. used the sample presented in Pace and Strigari 2018.
- For the dSph without photometric measurement of the J factor we take the prediction from their photo-J scaling relationship.
- The sample contains 48 dSphs.

Galaxy	L_V L_\odot	$r_{1/2}$ pc	d kpc	$J(0.5^\circ)$ $\text{GeV}^2 \text{cm}^{-5}$	Citation
Cetus II	8.6e1	17	30	19.1	a
Cetus III	8.2e2	44	251	17.2	b
Columba I	4.1e3	98	183	17.3	c
Grus II	3.1e3	93	53	18.4	a
Horologium II	94e2	33	78	18.3	d
Indus II	4.5e3	181	214	16.9	a
Pictor II	1.6e3	46	45	18.7	e
Pictoris I	2.6e3	43	126	17.9	f
Phoenix II	26e3	33	95	18.3	f
Reticulum III	1.8e3	64	92	18.0	a
Sagittarius II	1.0e4	33	67	18.7	g
Tucana IV	2.1e3	98	48	18.4	a
Tucana V	3.7e2	9.3	55	19.0	a
Virgo I	1.2e2	30	91	17.9	b

Galaxy	Distance kpc	$r_{1/2}$ pc	σ km s^{-1}	N	M_V	α_c deg	$J(0.1^\circ)$ $\text{GeV}^2 \text{cm}^{-5}$
Canes Venatici I	$210 \pm 6(\text{a})$	$424 \pm 25(\text{b})$	$7.6^{+0.5}_{-0.4}$	209(c)	-8.6 ± 0.15	0.232	$17.16^{+0.19}_{-0.18}$
Carina	$105.6 \pm 5.4(\text{d})$	$203 \pm 22(\text{e})$	$6.4^{+0.2}_{-0.2}$	758(f)	-9.1 ± 0.4	0.221	$17.66^{+0.16}_{-0.15}$
Draco	$76 \pm 6(\text{i})$	$182 \pm 13(\text{b})$	$9.1^{+0.3}_{-0.3}$	476(j)	-8.75 ± 0.15	0.276	$18.35^{+0.14}_{-0.11}$
Fornax	$147 \pm 9(\text{k})$	$609 \pm 38(\text{l})$	$10.6^{+0.2}_{-0.2}$	2409(f)	-13.4 ± 0.3	0.476	$17.90^{+0.12}_{-0.14}$
Leo I	$258.2 \pm 9.5(\text{m})$	$292 \pm 26(\text{n})$	$9.0^{+0.4}_{-0.4}$	327(o)	-12.0 ± 0.3	0.13	$17.36^{+0.12}_{-0.11}$
Leo II	$233 \pm 15(\text{p})$	$159 \pm 14(\text{q})$	$7.4^{+0.4}_{-0.4}$	175(r)	-9.9 ± 0.3	0.078	$17.63^{+0.19}_{-0.17}$
Sculptor	$83.9 \pm 1.5(\text{s})$	$230 \pm 36(\text{e})$	$8.8^{+0.2}_{-0.2}$	1349(f)	-11.04 ± 0.5	0.314	$18.30^{+0.14}_{-0.14}$
Sextans	$92.5 \pm 2.2(\text{t})$	$524 \pm 23(\text{u})$	$7.1^{+0.3}_{-0.3}$	424(f)	-9.1 ± 0.1	0.659	$17.37^{+0.24}_{-0.24}$
Ursa Minor	$76 \pm 4(\text{v})$	$201 \pm 23(\text{w})$	$9.3^{+0.4}_{-0.4}$	311(x)	-8.8 ± 0.5	0.305	$18.76^{+0.16}_{-0.20}$
Aquarius II	$107.9 \pm 3.3(\text{y})$	$123 \pm 22(\text{y})$	$6.2^{+2.6}_{-1.7}$	9(y)	-4.36 ± 0.14	0.131	$18.00^{+0.63}_{-0.59}$
Bootes I	$66 \pm 3(\text{z})$	$187 \pm 20(\text{b})$	$4.9^{+0.7}_{-0.6}$	37(aa)	-6.3 ± 0.2	0.325	$17.76^{+0.29}_{-0.28}$
Canes Venatici II	$160 \pm 7(\text{ab})$	$68 \pm 8(\text{ac})$	$4.7^{+1.2}_{-1.0}$	25(c)	-4.6 ± 0.2	0.049	$17.52^{+0.42}_{-0.41}$
Carina II	$37.4 \pm 0.4(\text{ad})$	$76 \pm 8(\text{ad})$	$3.4^{+1.2}_{-0.8}$	14(ae)	-4.4 ± 0.1	0.234	$17.86^{+0.56}_{-0.55}$
Coma Berenices	$42 \pm 1.5(\text{af})$	$57 \pm 4(\text{ag})$	$4.7^{+0.9}_{-0.8}$	58(c)	-3.9 ± 0.6	0.157	$18.59^{+0.31}_{-0.32}$
Draco II*	$20.0 \pm 3.0(\text{ah})$	$12 \pm 5(\text{ah})$	$3.4^{+2.5}_{-1.9}$	9(ai)	-2.9 ± 0.8	0.071	$18.60^{+1.29}_{-1.65}$
Grus I*	$120.2 \pm 11.1(\text{aj})$	$52 \pm 25(\text{aj})$	$4.5^{+5.0}_{-2.8}$	5(ak)	-3.4 ± 0.3	0.05	$16.64^{+1.30}_{-1.68}$
Hercules	$132 \pm 6(\text{al})$	$106 \pm 13(\text{am})$	$3.9^{+1.3}_{-1.0}$	30(c)	-6.6 ± 0.3	0.092	$17.11^{+0.31}_{-0.51}$
Horologium I	$87 \pm 8(\text{an})$	$32 \pm 5(\text{an})$	$5.9^{+3.3}_{-1.8}$	5(ao)	-3.5 ± 0.3	0.047	$19.00^{+0.76}_{-0.63}$
Horologium I	$79 \pm 7(\text{aj})$	$60 \pm 35(\text{aj})$	$5.9^{+3.3}_{-1.8}$	5(ao)	-3.4 ± 0.1	0.079	$18.59^{+0.86}_{-0.78}$
Hydra II	$151 \pm 8(\text{ap})$	$71 \pm 11(\text{aq})$	< 6.82	13(ar)	-5.1 ± 0.3	0.054	< 17.51
Leo IV*	$154 \pm 5(\text{as})$	$111 \pm 36(\text{at})$	$3.4^{+2.0}_{-1.8}$	17(c)	-4.92 ± 0.2	0.083	$16.28^{+0.94}_{-1.18}$
Leo V*	$173 \pm 5(\text{au})$	$30 \pm 16(\text{ac})$	$4.9^{+3.0}_{-1.9}$	8(av)	-4.1 ± 0.4	0.02	$17.53^{+0.89}_{-0.96}$
Pegasus III*	$215 \pm 12(\text{aw})$	$37 \pm 14(\text{aw})$	$7.9^{+4.4}_{-3.1}$	7(aw)	-3.4 ± 0.4	0.02	$18.25^{+0.84}_{-0.60}$
Pisces II*	$183 \pm 15(\text{ac})$	$48 \pm 10(\text{ac})$	$4.8^{+3.3}_{-2.0}$	7(ar)	-4.1 ± 0.4	0.03	$17.15^{+0.95}_{-1.08}$
Reticulum II	$32 \pm 2(\text{an})$	$34 \pm 8(\text{an})$	$3.4^{+0.7}_{-0.6}$	25(ax)	-3.6 ± 0.1	0.121	$18.47^{+0.36}_{-0.34}$
Reticulum II	$30 \pm 2(\text{aj})$	$32 \pm 3(\text{aj})$	$3.4^{+0.7}_{-0.6}$	25(ax)	-2.7 ± 0.1	0.121	$18.55^{+0.35}_{-0.33}$
Segue 1	$23 \pm 2(\text{ay})$	$21 \pm 5(\text{b})$	$3.1^{+0.9}_{-0.8}$	62(az)	-1.5 ± 0.7	0.103	$18.85^{+0.55}_{-0.60}$
Segue 2	$36.6 \pm 2.45(\text{ba})$	$33 \pm 3(\text{bb})$	< 3.20	25(bc)	-2.6 ± 0.1	0.103	< 17.84
Triangulum II	$30 \pm 2(\text{bd})$	$28 \pm 8(\text{bd})$	< 6.36	13(be)	-1.8 ± 0.5	0.109	< 19.36
Tucana II	$57.5 \pm 5.3(\text{aj})$	$162 \pm 35(\text{aj})$	$7.3^{+2.6}_{-1.7}$	10(ak)	-3.8 ± 0.1	0.325	$18.42^{+0.57}_{-0.50}$
Tucana II	$57.5 \pm 5.3(\text{an})$	$115 \pm 32(\text{an})$	$7.3^{+2.6}_{-1.7}$	10(ak)	-3.9 ± 0.2	0.232	$18.64^{+0.60}_{-0.55}$
Tucana III	$25 \pm 2(\text{bf})$	$43 \pm 6(\text{bf})$	< 2.18	26(bg)	-2.4 ± 0.2	0.2	< 17.31
Ursa Major I	$97.3 \pm 5.85(\text{bh})$	$200 \pm 21(\text{bi})$	$7.3^{+1.2}_{-1.0}$	36(c)	-5.5 ± 0.3	0.236	$17.94^{+0.34}_{-0.32}$
Ursa Major II	$34.7 \pm 2.1(\text{bj})$	$99 \pm 7(\text{ag})$	$7.2^{+1.8}_{-1.4}$	19(c)	-4.2 ± 0.5	0.327	$18.99^{+0.45}_{-0.41}$
Willman 1	$38 \pm 7(\text{bk})$	$18 \pm 4(\text{b})$	$4.5^{+1.0}_{-0.8}$	40(bl)	-2.7 ± 0.7	0.056	$19.18^{+0.47}_{-0.44}$
Cetus	$780 \pm 40(\text{bm})$	$497 \pm 37(\text{bn})$	$8.2^{+0.8}_{-0.7}$	116(bo)	-10.1 ± 0.0	0.073	$16.20^{+0.21}_{-0.19}$
Eridanus II	$366 \pm 17(\text{bp})$	$176 \pm 14(\text{bp})$	$7.1^{+1.2}_{-0.9}$	28(bq)	-7.1 ± 0.3	0.055	$17.14^{+0.29}_{-0.26}$
Leo T	$407 \pm 38(\text{br})$	$142 \pm 36(\text{b})$	$7.9^{+2.0}_{-1.5}$	19(c)	-7.1 ± 0.0	0.04	$17.35^{+0.45}_{-0.42}$
And I	$727 \pm 17.5(\text{bs})$	$699 \pm 29(\text{bt})$	$10.9^{+2.3}_{-1.7}$	51(bu)	-11.2 ± 0.2	0.11	$16.68^{+0.37}_{-0.36}$
And III	$723 \pm 21(\text{bs})$	$296 \pm 33(\text{bt})$	$9.8^{+1.5}_{-1.3}$	62(bu)	-9.5 ± 0.3	0.047	$16.85^{+0.29}_{-0.27}$
And V	$742 \pm 21.5(\text{bs})$	$294 \pm 33(\text{bt})$	$11.0^{+1.2}_{-1.0}$	85(bu)	-9.3 ± 0.2	0.045	$17.11^{+0.23}_{-0.21}$
And VII	$763 \pm 35(\text{bv})$	$717 \pm 39(\text{bn})$	$13.3^{+1.0}_{-1.0}$	136(bu)	-12.2 ± 0.0	0.108	$16.89^{+0.17}_{-0.17}$
And XIV	$793 \pm 50(\text{bs})$	$297 \pm 53(\text{bt})$	$5.9^{+1.0}_{-0.9}$	48(bu)	-8.5 ± 0.35	0.043	$15.65^{+0.37}_{-0.38}$
And XVIII	$1214 \pm 41.5(\text{bs})$	$260 \pm 38(\text{bt})$	$10.5^{+2.8}_{-2.1}$	22(bu)	-9.2 ± 0.35	0.025	$16.70^{+0.46}_{-0.43}$

Analysis of the dSphs



Dark matter limits derived from the GeV excess

- Excesses found at other locations along the Galactic plane.
- We have derived limits for the **annihilation cross section** as a function of the **DM mass**.
- If DM exists \longrightarrow γ -ray emission from dwarf spheroidal satellite galaxies of the Milky Way.

